[redacted]

233

[redacted]

Copy
RM L56J17

NACA RM L56J17

Reg# 1175
JAN 16
0144208
TECH LIBRARY KAFB, NM

NACA

RESEARCH MEMORANDUM

7729

HINGE-MOMENT AND EFFECTIVENESS CHARACTERISTICS OF AN ASPECT-RATIO-8.2 FLAP-TYPE CONTROL ON A 60° DELTA WING AT MACH NUMBERS FROM 0.72 TO 1.96

By Lawrence D. Guy

Langley Aeronautical Laboratory
Langley Field, Va.

[redacted]

[redacted]

NATIONAL ADVISORY COMMITTEE
FOR AERONAUTICS

WASHINGTON

January 7, 1957

[redacted]

[redacted]

TECH LIBRARY KAFB, NM
0144208

NATIONAL ADVISORY COMMITTEE FOR AERONAUTICS

RESEARCH MEMORANDUM

HINGE-MOMENT AND EFFECTIVENESS CHARACTERISTICS OF AN ASPECT-RATIO-8.2 FLAP-TYPE CONTROL ON A 60° DELTA WING AT MACH NUMBERS FROM 0.72 TO 1.96

By Lawrence D. Guy

SUMMARY

An investigation of a semispan-wing—fuselage model having a 60° delta wing with an aspect-ratio-8.2 blunt trailing-edge flap-type control was conducted in the Langley 9- by 12-inch blowdown tunnel. Control hinge-moment and effectiveness characteristics were obtained over an angle-of-attack range of ±10° at control deflections up to 90°. At the highest deflection the control could be considered as a spoiler. Data were obtained at Mach numbers from 0.72 to 1.96.

The control showed positive effectiveness in lift and rolling moment throughout the Mach number, angle-of-attack and control-deflection range of the investigation. At small deflections the effectiveness (based on control moment areas) was at least as great as that of a more conventional aspect-ratio-4.4 sharp trailing-edge control. At moderate angles of attack with the controls acting as ailerons deflected to produce a given roll rate, the magnitude of the hinge moments for the high-aspect-ratio control were much smaller than for the aspect-ratio-4.4 control of NACA RM L54G12a at all speeds and showed less change with Mach number at transonic speeds. This result was in agreement with the theoretical analysis of minimum hinge-moment controls presented in NACA TN 3471 and also illustrates the advantage of using small controls with large deflections to obtain low hinge moments for a given rate of roll.

INTRODUCTION

At supersonic speeds the magnitude of control forces on airplanes and missiles is such as to require large power-boost systems that add to the size, weight, and complexity of the aircraft. A need therefore exists for reduction of the control forces by aerodynamic means. One approach to a solution of this problem has been made in reference 1

wherein various unbalanced trailing-edge controls were analyzed theoretically to determine those having minimum hinge moments due to deflection at supersonic speeds. This analysis indicated that, when the required control size and plan form is not restrictive, maximum ratios of lift to hinge moments are obtained with untapered high-aspect-ratio controls. Also, for a given control shape the importance of using small controls with high deflections for obtaining large ratios of rolling moment to hinge moment was illustrated. At transonic speeds, experimental evidence (ref. 2) has indicated that small chord controls may have hinge moments less affected by compressibility than the more conventional types. In order to obtain information on these premises, a 60° delta wing equipped with an aspect-ratio-8.2 untapered control has been investigated at transonic and supersonic speeds in the Langley 9- by 12-inch blowdown tunnel. The control was located at the wing trailing edge and had an unswept hinge line.

Hinge-moment and effectiveness characteristics of the control were obtained for an angle-of-attack range of ±10° at Mach numbers from 0.72 to 1.96. Control deflections up to 90° were investigated to determine the behavior of the control as a trailing-edge spoiler. The average Reynolds number of the investigation varied between about 2.4×10^6 and 3.4×10^6.

SYMBOLS

The measured aerodynamic forces and moments were reduced to standard nondimensional coefficients and were referred in all cases to the wind axes.

A	aspect ratio
b	wing span, twice distance from rolling-moment reference axis to wing tip
b_f	control-surface span
c	local wing chord
$\bar{c}$	mean aerodynamic chord of wing
c_f	control chord behind the hinge line
$\bar{c}_f$	mean aerodynamic chord of portion of control behind hinge line
$c_{f,1}$	value of c_f for control of reference 3

C_D drag coefficient, $\frac{\text{Drag}}{qS}$

ΔC_D increment in drag coefficient due to angle of attack and/or control deflection

C_h control hinge-moment coefficient, $\frac{\text{Hinge moment}}{qb_f\bar{c}_f^2}$

$C_l, \Delta C_L, \Delta C_m$ increments in gross rolling-moment coefficient, lift coefficient, and pitching-moment coefficient, respectively, due to deflection of control surface

$C_{l,gross}$ gross rolling-moment coefficient (rolling-moment reference axis shown in fig. 1), $\frac{\text{Rolling moment}}{2qSb}$

C_L lift coefficient, $\frac{\text{Lift}}{qS}$

C_m pitching-moment coefficient (pitching-moment reference axis located at $0.25\bar{c}$), $\frac{\text{Pitching moment}}{qS\bar{c}}$

h projection of control trailing edge from wing surface at hinge line in direction normal to wing-chord plane (positive trailing edge down)

M Mach number

ΔM maximum deviation from average test-section Mach number

q free-stream dynamic pressure

R Reynolds number based on mean aerodynamic chord of wing

S semispan wing area (including area blanketed by half-body of revolution)

W deflection work, $2qb_f\bar{c}_f^2\left[\int_0^{\delta} C_h d\left(\frac{\delta}{57.3}\right) + \int_0^{-\delta} C_h d\left(\frac{\delta}{57.3}\right)\right]$

$\bar{x}$ chordwise center-of-pressure location of ΔC_L

α angle of attack measured with respect to free stream

δ control-surface deflection measured perpendicular to hinge line from wing-chord plane (positive trailing edge down), deg

Subscripts:

α	partial derivative of coefficient with respect to α
δ	partial derivative of coefficient with respect to δ
f	flap

DESCRIPTION OF MODEL

The principal dimensions of the semispan-wing—body combination are given in figure 1. The wing had a delta plan form with 60° leading-edge sweepback and a corresponding aspect ratio of 2.31. The main wing panel, exclusive of the control surface, was of solid steel and had 4-percent-thick hexagonal airfoil sections modified at the leading and trailing edge by a small radius. A body consisting of a half-body of revolution together with 0.25-inch shim was integral with the main wing panel for all tests.

The constant-chord partial-span control surface was located at the wing trailing edge such that the control inboard end was adjacent to the fuselage and the control extended spanwise to about $0.65b/2$. The control was machined of heat-treated steel and had a constant thickness of $0.0084\bar{c}$. The control was hinged to the main wing panel by a 0.040-inch-diameter steel pin at the outboard end. At the inboard end, a 0.109-inch-diameter shaft machined integral with the control surface was supported by a bearing within the test body and restrained by a clamp.

TEST TECHNIQUE

The semispan model was cantilevered from a five-component strain-gage balance which mounts flush with the tunnel floor and rotates with the model through the angle-of-attack range. The aerodynamic forces and moments on the semispan wing-body combination were measured with respect to the body axes and then transferred to the wind axes. The 0.25-inch shim was used to minimize the effects of the tunnel-wall boundary layer on the flow over the fuselage (refs. 4 and 5). A clearance gap of 0.010 to 0.020 inch was maintained between the fuselage shim and the tunnel floor.

Control-surface hinge moments were measured by means of an electrical-strain-gage beam which formed a part of the clamp restraining the control-surface shaft and which was contained within the test body. For all tests the Mach number and control deflection were preset and the angle of attack was varied.

TUNNEL AND TEST CONDITIONS

The tests were conducted in the Langley 9- by 12-inch blowdown tunnel which operated from the compressed air of the Langley 19-foot pressure tunnel. The absolute stagnation pressure of the air entering the test section ranged from 2 to $2\frac{1}{3}$ atmospheres. The compressed air was conditioned to insure condensation-free flow in the test section by being passed through a silica-gel drier and then through banks of finned electrical heaters. Criteria for condensation-free flow were obtained from reference 6. Turbulence damping screens were located in the settling chamber. Four interchangeable nozzle blocks provided test-section Mach numbers of 0.70 to 1.20, 1.41, 1.62, and 1.96.

Transonic Nozzle

A description of the transonic nozzle, which has a 7- by 10-inch test section, together with a discussion of the flow characteristics obtained from limited calibration tests is presented in reference 3. Satisfactory test-section flow characteristics are indicated from the minimum Mach number ($M \approx 0.7$) to about $M = 1.2$. With the tunnel clear the maximum deviations from the average Mach number in the region occupied by the model are shown in figure 2(a). Limited tests indicate that the stream angle probably did not exceed $\pm 0.1^{\circ}$ at any Mach number. During tests the test-section flow was maintained within ± 0.005 of the desired Mach number by an electronically modulated device. The variation with Mach number of the average Reynolds number of the tests is given in figure 2(b).

Supersonic Nozzles

Test-section flow characteristics of the three supersonic fixed Mach number nozzles, which had 9- by 12-inch test sections, were determined from extensive calibration tests and are reported in reference 7. Deviation of flow conditions in the test section with the tunnel clear are presented in the following table:

Average Mach number	1.41	1.62	1.96
Maximum deviation in Mach number	±0.02	±0.01	±0.02
Maximum deviation in stream angle, deg . . .	±0.25	±0.20	±0.20
Average Reynolds number (approximate) . .	3.0×10^6	2.7×10^6	2.4×10^6

ACCURACY AND LIMITATION OF DATA

An estimate of the probable errors introduced in the present data by instrument reading errors and measuring equipment errors are presented in the following table:

Variable	Error
C_L	±0.005
C_l	±.0005
C_m	±.001
C_D	±.001
C_h	±.01
α, deg	±.1
δ, deg	±.2

The error in δ is the estimated error in the no-load control setting. Corrections for the change in deflection due to control hinge moments were determined from static hinge-moment calibrations and applied to the measured no-load control setting.

Corrections are not available for the transonic nozzle to allow for jet boundary interference and blockage at transonic speeds or for reflection-plane effects at high subsonic speeds. Furthermore, shock and expansion-wave reflection interference exists at low supersonic speeds. This imposes certain limitations on the data, particularly the loadings due to angle of attack, which are discussed in references 3 and 8. In general, however, the wing and control characteristics due to angle of attack with the exception of drag are believed to be reliable except between Mach numbers 0.94 and 1.04, whereas the control characteristics due to deflection are believed to be reliable at all Mach numbers presented. For detailed discussion, see references 3 and 8. In the fixed Mach number nozzles ($M = 1.41$ and higher), the models were clear of wall-reflected disturbances.

RESULTS AND DISCUSSION

Aerodynamic characteristics of the semispan model are presented in figures 3 and 4 as functions of the flap deflection for Mach numbers from 0.72 to 1.96. The rolling-moment coefficients and increments in lift and pitching-moment coefficients due to flap deflection obtained from the figures are plotted in figure 5 for a few representative Mach

numbers. The basic hinge-moment data are plotted against flap deflection for all Mach numbers in figure 6 and cross plotted against angle of attack in figure 7 for the selected Mach numbers. For these figures the data were obtained at control deflections from -5° to 90° at both positive and negative angles of attack. For convenience of presentation, the signs of the test values of angle of attack, control deflection, and model force and moment coefficients obtained at negative angles of attack have been arbitrarily reversed. This reversal was permissible by reason of model symmetry.

The zero-lift drag values of the present tests have little value, principally because of the presence of the boundary-layer shim on the test body and have therefore been subtracted from all drag coefficients presented in figure 4. The values of the incremental drag coefficients due to angle of attack are of questionable reliability at transonic speeds because of boundary-interference effects (see ref. 8); the drag-coefficient increments due to control deflection, however, were believed to have been unaffected.

No corrections are available to allow for reflection-plane interference at subsonic and low supersonic Mach numbers. Consequently some error in the absolute values of C_l, ΔC_L, and ΔC_h indicated for differentially deflected ailerons is introduced. The error in differences of comparative values, however, is believed small.

Flap Characteristics

Flap effectiveness.- As shown in figure 5 the control was effective in producing rolling moment, lift, and pitching moment to high deflections and moderate angles of attack throughout the Mach number range from 0.72 to 1.96. The slopes of the curves were a maximum at zero deflection and generally decreased to zero at 90° deflection as would be expected. At subsonic speeds deflecting the control from 0° to 20° caused approximately a 50-percent loss in lift and rolling-moment effectiveness (rate of change of coefficient with deflection). At supersonic speeds, although the initial effectiveness was much smaller, the control could be deflected from 0° to 30° or 40° before a 50-percent loss in effectiveness was incurred.

The effect of Mach number on the initial control rolling effectiveness $\left(C_{l_\delta} \text{ at } \delta = 0^{\circ}\right)$ is shown in figure 8. Figure 8 shows a rapid loss in effectiveness at transonic speeds followed by a more gradual reduction in values of C_{l_δ} at supersonic speeds to about 10 percent of the subsonic values. Also shown in figure 8 are values of C_{l_δ} obtained from reference 3 for a similar unbalanced control on the same wing-fuselage

model as that of the present paper. The control of reference 3 had the same span and spanwise location as that of the present paper but differed in having approximately twice the chord (half the aspect ratio) and a 6° trailing-edge angle as compared with 0° for the present flap. In the discussion to follow the control of the present report will be referred to as the high-aspect-ratio control or flap. Figure 8 shows that the larger control ($A = 4.4$) had larger values of C_{l_δ} throughout the speed range. However, normalizing the values of C_{l_δ} on the basis of control area (the span and moment arm were the same for both controls) would increase the effectiveness of the high-aspect-ratio control relative to that of the $A = 4.4$ control by a factor of 1.9. On this basis, the effectiveness for the $A = 4.4$ control would be 70 percent of that of the $A = 8.2$ control at $M = 0.80$, 75 percent at $M = 1.0$, and essentially equal effectiveness at Mach numbers from 1.2 to 2.0. The decreased trailing-edge angle of the full blunt $A = 8.2$ control undoubtedly contributes part of the increase in effectiveness throughout most of the speed range but particularly at the transonic speeds (ref. 9). At supersonic speeds comparison of experiment with linear theory (not including thickness effects, ref. 10) shows approximately the same relative values at $M = 1.3$ for both controls with experimental values about 70 percent of the theoretical values. At the highest Mach number, the experimental values of C_{l_δ} have decreased to 65 percent of theory for the $A = 4.4$ control but have decreased to nearly 55 percent of theory for the high-aspect-ratio control. Thus, at the highest Mach numbers part of the advantages of the high-aspect-ratio control predicted by reference 1 are not realized.

Flap hinge moments.- The variation of hinge-moment coefficients with flap deflection was linear with negative slopes over a range of control deflections that varied from about $\pm 20^{\circ}$ at subsonic speeds to about $\pm 10^{\circ}$ at supersonic speeds (fig. 6). At slightly greater deflections a moderate decrease in lift-curve slope followed by a less rapid decrease in slope with increasing deflection up to the maximum of the tests occurred. The most rapid changes in slope occurred near a Mach number of 1.0. It is noteworthy that maximum hinge-moment coefficients are not, in general, necessarily approached in all cases as the deflection approaches $\pm 90^{\circ}$. In fact, at subsonic Mach numbers the slope of the curve of the hinge-moment coefficient plotted against the control deflection was still negative in sign and of appreciable magnitude at $\pm 90^{\circ}$. This behavior suggests three possibilities: (1) stagnation conditions were not fully established on the forward face of the control at 90° deflection, (2) the blunt trailing edge of the control was contributing actively to the hinge moments at deflections near 90° and larger, (3) aeroelastic effects produced bending and twisting deflection of the flap. Although the narrow chord of the flap relative to its span would make the third explanation appear feasible, the hinge-moment curve slopes at 90° are less negative or zero at higher Mach numbers where the dynamic pressure was greater.

The variations of hinge-moment coefficient with angle of attack (fig. 7) show some nonlinearities at negative flap deflections throughout the speed range of the tests. At positive deflections, however, the variations were nearly linear with negative slope for most of the speed range.

Figure 8 presents the hinge-moment parameters C_{h_α} and C_{h_δ} as a function of Mach number for both the present control and the lower aspect-ratio control of reference 3. Values of C_{h_α}, however, were slightly larger in magnitude for the high-aspect-ratio control than for the $A = 4.4$ control at subsonic and transonic speeds. Close agreement is shown in values of C_{h_δ} for the two controls. Linear theory shows slightly greater values of C_{h_δ} for the $A = 8.2$ control at supersonic speeds. This is not entirely borne out by experiment; however, the differences are of the order of magnitude of the experimental accuracy. The possibility of small chord controls having less effect of compressibility on control hinge moments was not realized. It appears, therefore, such effects noted in reference 2 for an inset tab were due to other factors, possibly the sweep (forward) of the control hinge line and trailing edge.

Evaluation of control effectiveness.- Figures 9 and 10 are presented to aid the evaluation of the characteristics of the high-aspect-ratio control under practical conditions. The upper plot of figure 9 presents, as a function of Mach number, the values of C_l estimated to be required to produce an arbitrary roll rate of the subject wing of 3.5 radians per second (a 30-foot wing span being assumed at an altitude of 40,000 feet). The values were calculated by use of theoretical values of C_{l_p} from references 11 and 12. The lower plots of figure 9 present the experimental values of $C_h\left(\frac{c_f^2}{c_{f,1}^2}\right)$ against Mach number for equal up and down deflection of opposite ailerons which would produce the calculated required rolling moment. The parameter $C_h\left(\frac{c_f^2}{c_{f,1}^2}\right)$ is used in this figure to afford a direct comparison of the hinge moments for the aspect-ratio-8.2 control of the present paper and the aspect-ratio-4.4 unbalanced control of reference 3. Data are shown for the steady roll and static cases. Data for the static case are representative of the condition in which the controls are fully deflected before the aircraft starts to roll. The analysis by which the data were obtained is discussed in detail in reference 13.

Values of the hinge-moment parameter of figure 9 are shown for the aspect-ratio-8.2 and aspect-ratio-4.4 controls at $\alpha = 0^\circ$ and $\alpha = 8^\circ$. These data indicate smaller values of hinge moment throughout the speed

range for the higher aspect-ratio control. The incremental change in the hinge-moment parameter at transonic speeds was of the order of twice the subsonic value for both controls; however, the magnitude of the increment was smaller for the high-aspect-ratio control. At supersonic speeds the data support the analysis of reference 1 which indicated that high-aspect-ratio untapered controls would possess maximum ratios of rolling moment to hinge moment. In general, the data illustrate the advantage of using small controls with large deflections to obtain low hinge moments for a given rate of roll. Correspondingly less torque would be required to be available at the control and the strength and weight of the actuating mechanism could be reduced.

The work required to overcome the hinge moments due to deflection is also an important consideration, since it determines the amount of energy which must be supplied to the power-boost system. A comparison on the basis of deflection work for the two controls producing the above roll rate is presented in figure 10 at angles of attack of 0° and 8°. These data show little difference in the deflection work for the two controls throughout the speed range at both angles of attack. These results indicate no penalty for using the larger required deflections for the smaller control to produce the stated roll rate.

Spoiler Characteristics

Figures 11 to 13 present the aerodynamic characteristics of the aspect-ratio-8.2 control as a function of the projection of the control normal to the wing surface. In these figures the control is assumed to behave as a spoiler since at an up or down deflection of 90° the control may be considered as a spoiler located at 94.8 percent $\bar{c}$ or as a trailing-edge spoiler. In either case no surface exists downstream of the spoiler to carry loading of opposite sense to that desired. In order to avoid confusion, the spoiler notation employs the same sign convention used for trailing-edge flaps throughout this report; that is, the deflection is positive when the trailing edge is down (spoiler projecting from the wing lower surface).

Figure 11 shows that the curves of the variation of rolling moment and increments in lift and pitching-moment coefficients with projection approach a parabolic shape at subsonic speeds. At supersonic speeds the curves generally become more nearly linear with projection. Conversely, the hinge-moment-coefficient curves are nearly linear at subsonic speeds but show larger changes in slope with projection at supersonic speeds. As previously noted, the hinge-moment-coefficient curves show some effects of control thickness near maximum projection at subsonic speeds.

The chordwise centers of pressure of the incremental lift due to projection were calculated from the force and moment data and are shown

as a function of angle of attack for three Mach numbers in figure 12. Data are shown for the control deflected 10° ($h/\bar{c}$ = 0.01) and 90° ($h/\bar{c}$ = 0.052) to indicate the differences in wing loading due to flap-type and spoiler-type controls, that is, for the cases of nonseparated and separated flow on the wing ahead of the control. It should be kept in mind that the incremental-lift values in each case were, of course, different and also that the control trailing edge was $0.04\bar{c}$ farther downstream at 10° deflection than at 90° deflection. The variations of center-of-pressure position with angle of attack are nonlinear for both the flap-type and spoiler-type loadings. The spoiler centers of pressure were approximately $0.06\bar{c}$ farther forward than those for the flap. This is shown more clearly in figure 13 which shows the variation with Mach number of the center-of-pressure location of the incremental lift due to deflection at angles of attack of 0° and 8°. In general, the same trends are shown as in reference 14. At an angle of attack of 0° the chordwise centers of pressure moved rearward much less rapidly at transonic speeds for the spoilers than for the flap. At an angle of attack of 8°, however, the center-of-pressure shift was as abrupt for the spoiler as for the flap. The center-of-pressure locations for the spoiler were 6 to 10 percent forward of that for the flap at all Mach numbers. Data at positive deflections and low supersonic Mach numbers were not obtained because of load limitations on the balance.

CONCLUSIONS

An investigation of a 60° delta-wing—fuselage combination with an aspect-ratio-8.2 constant-chord blunt trailing-edge control in the Langley 9- by 12-inch blowdown tunnel at Mach numbers from 0.72 to 1.96 indicated the following conclusions:

1. The control showed positive effectiveness in lift and rolling moment throughout the range of the investigation including angles of attack of ±10° and control deflections up to 90°.

2. Comparison with a more conventional aspect-ratio-4.4 control, having twice the chord length and a sharp trailing-edge angle, showed that the rolling-moment-coefficient effectiveness (based on the control moment areas) for the full blunt high-aspect-ratio control was greater at subsonic and transonic speeds and equal to that of the lower aspect-ratio control at supersonic speeds.

3. At moderate angles of attack with the controls deflected to produce a given roll rate, the magnitude of the hinge moments for the high-aspect-ratio control was much smaller than that for the aspect-ratio-4.4 control of NACA RM L54G12a at all speeds and showed less change with Mach number at transonic speeds. This result was in agreement with the

theoretical analysis of minimum hinge-moment controls presented in NACA TN 3471 and also illustrates the advantage of using small controls with large deflections to obtain low hinge moments for a given rate of roll.

4. Comparison of the two controls on the basis of deflection work for the same roll rate showed no penalty for the smaller control because of the larger required deflections.

Langley Aeronautical Laboratory,
National Advisory Committee for Aeronautics,
Langley Field, Va., September 28, 1956.

REFERENCES

1. Goin, Kennith L.: Theoretical Analysis To Determine Unbalanced Trailing-Edge Controls Having Minimum Hinge Moments Due to Deflection at Supersonic Speeds. NACA TN 3471, 1955. (Supersedes NACA RM L51F19.)

2. Smith, Donald W., and Reed, Verlin D.: Subsonic Static Longitudinal Stability and Control Characteristics of a Wing-Body Combination Having a Pointed Wing of Aspect Ratio 2 with Constant-Percent-Chord Trailing-Edge Elevons. NACA RM A53C20, 1953.

3. Guy, Lawrence D.: Effects of Overhang Balance on the Hinge-Moment and Effectiveness Characteristics of an Unswept Trailing-Edge Control on a 60° Delta Wing at Transonic and Supersonic Speeds. NACA RM L54G12a, 1954.

4. Conner, D. William: Aerodynamic Characteristics of Two All-Movable Wings Tested in the Presence of a Fuselage at a Mach Number of 1.9. NACA RM L8H04, 1948.

5. Mitchell, Meade H., Jr.: Effects of Varying the Size and Location of Trailing-Edge Flap-Type Controls on the Aerodynamic Characteristics of an Unswept Wing at a Mach Number of 1.9. NACA RM L50F08, 1950.

6. Burgess, Warren C., Jr., and Seashore, Ferris L.: Criterions for Condensation-Free Flow in Supersonic Tunnels. NACA TN 2518, 1951.

7. May, Ellery B., Jr.: Investigation of the Effects of Leading-Edge Chord-Extensions on the Aerodynamic and Control Characteristics of Two Sweptback Wings at Mach Numbers of 1.41, 1.62, and 1.96. NACA RM L50L06a, 1951.

8. Guy, Lawrence D., and Hadaway, William M.: Aerodynamic Loads on an External Store Adjacent to a 45° Sweptback Wing at Mach Numbers From 0.70 to 1.96, Including an Evaluation of Techniques Used. NACA RM L55H12, 1955.

9. Strass, H. Kurt, Stephens, Emily W., Fields, Edison M., and Schult, Eugene D.: Collection and Summary of Flap-Type-Aileron Rolling-Effectiveness Data at Zero Lift As Determined by Rocket-Powered Model Tests at Mach Numbers Between 0.6 and 1.6. NACA RM L55F14, 1955.

10. Lagerstrom, P. A., and Graham, Martha E.: Linearized Theory of Supersonic Control Surfaces. Jour. Aero. Sci., vol. 16, no. 1, Jan. 1949, pp. 31-34.

11. Polhamus, Edward C.: A Simple Method of Estimating the Subsonic Lift and Damping in Roll of Sweptback Wings. NACA TN 1862, 1949.

12. Malvestuto, Frank S., Jr., Margolis, Kenneth, and Ribner, Herbert S.: Theoretical Lift and Damping in Roll at Supersonic Speeds of Thin Sweptback Tapered Wings With Streamwise Tips, Subsonic Leading Edges, and Supersonic Trailing Edges. NACA Rep. 970, 1950. (Supersedes NACA TN 1860.)

13. Goin, Kennith L., and Palmer, William E.: Subsonic and Supersonic Hinge-Moment and Effectiveness Characteristics of an Unbalanced Lateral Control Having Low Theoretical Hinge Moments at Supersonic Speeds. NACA RM L53G31a, 1953.

14. Hammond, Alexander D.: Loads on Wings Due to Spoilers at Subsonic and Transonic Speeds. NACA RM L55E17a, 1955.

[redacted]

Fuselage ordinates	
Station	Radius
0	0
.541	.094
1.082	.180
1.623	.260
2.165	.330
2.706	.391
3.247	.444
3.788	.490
4.330	.519
4.870	.538
5.412	.541
10.000	.541

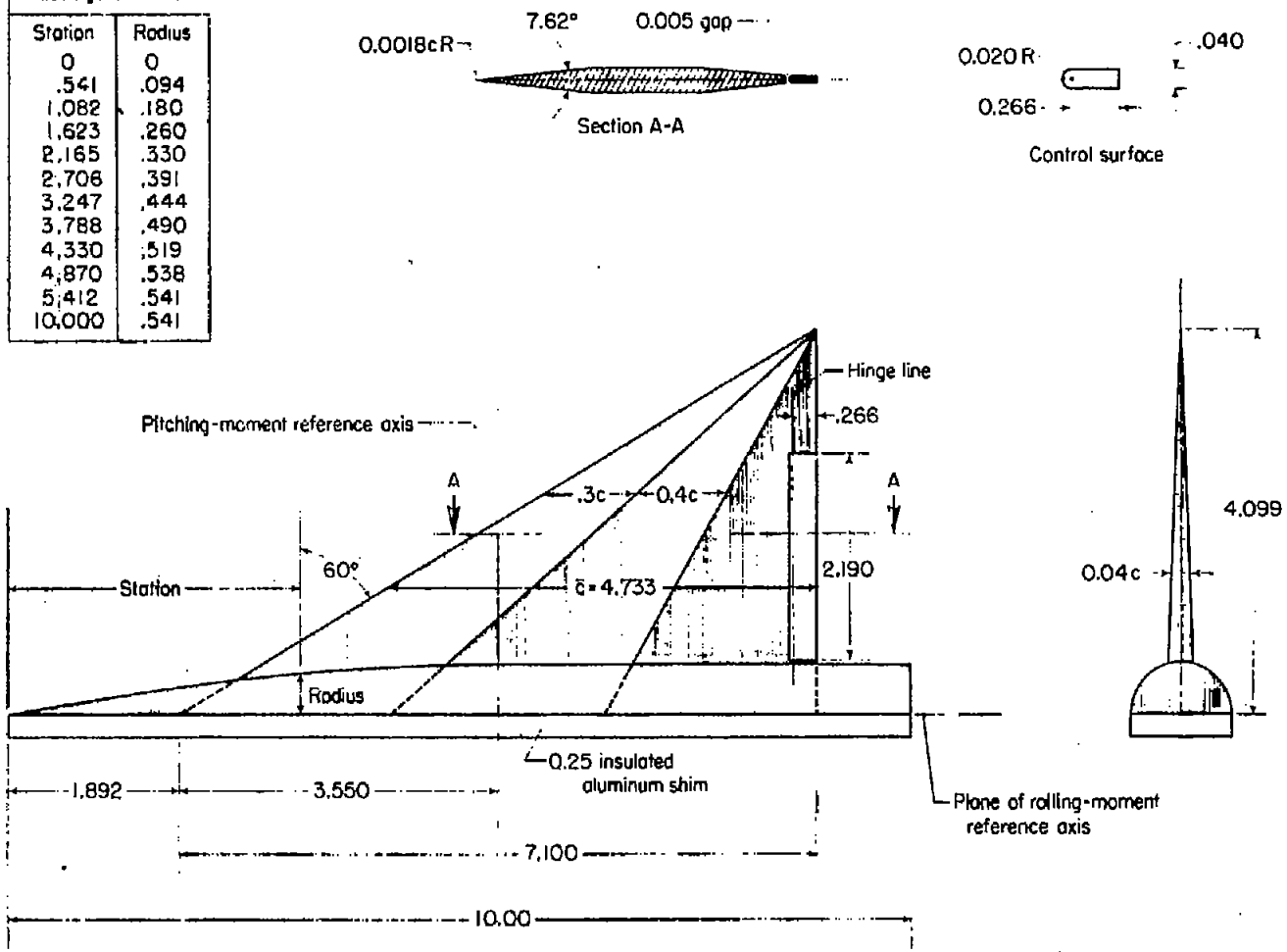

Figure 1.- Details of semispan-wing - fuselage combination. Semispan, 4.099 inches; semispan-wing area, 14.522 square inches. All dimensions are in inches.

[redacted]

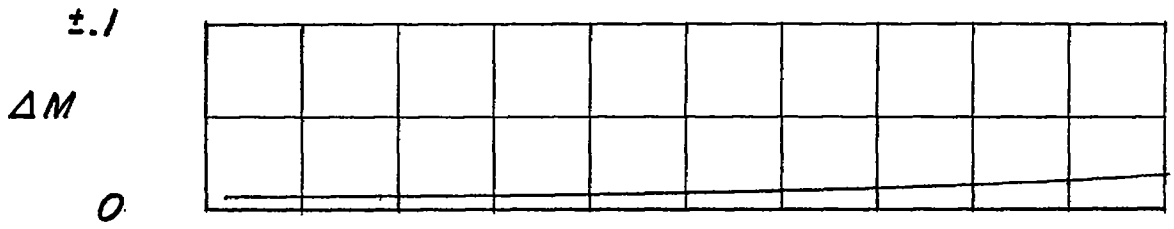

(a) Maximum deviation from average test section Mach number.

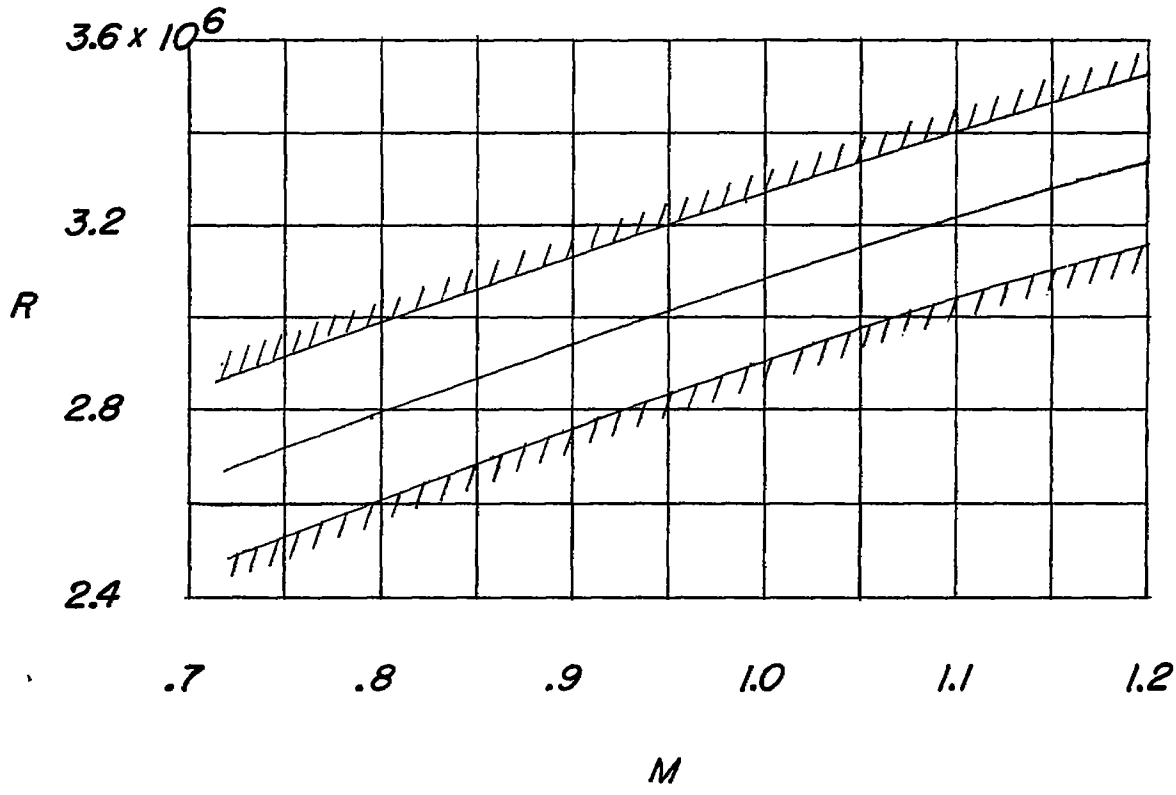

(b) Test Reynolds number based on wing mean aerodynamic chord.

Figure 2.- Test-section Mach number and Reynolds number characteristics of the transonic nozzle and model.

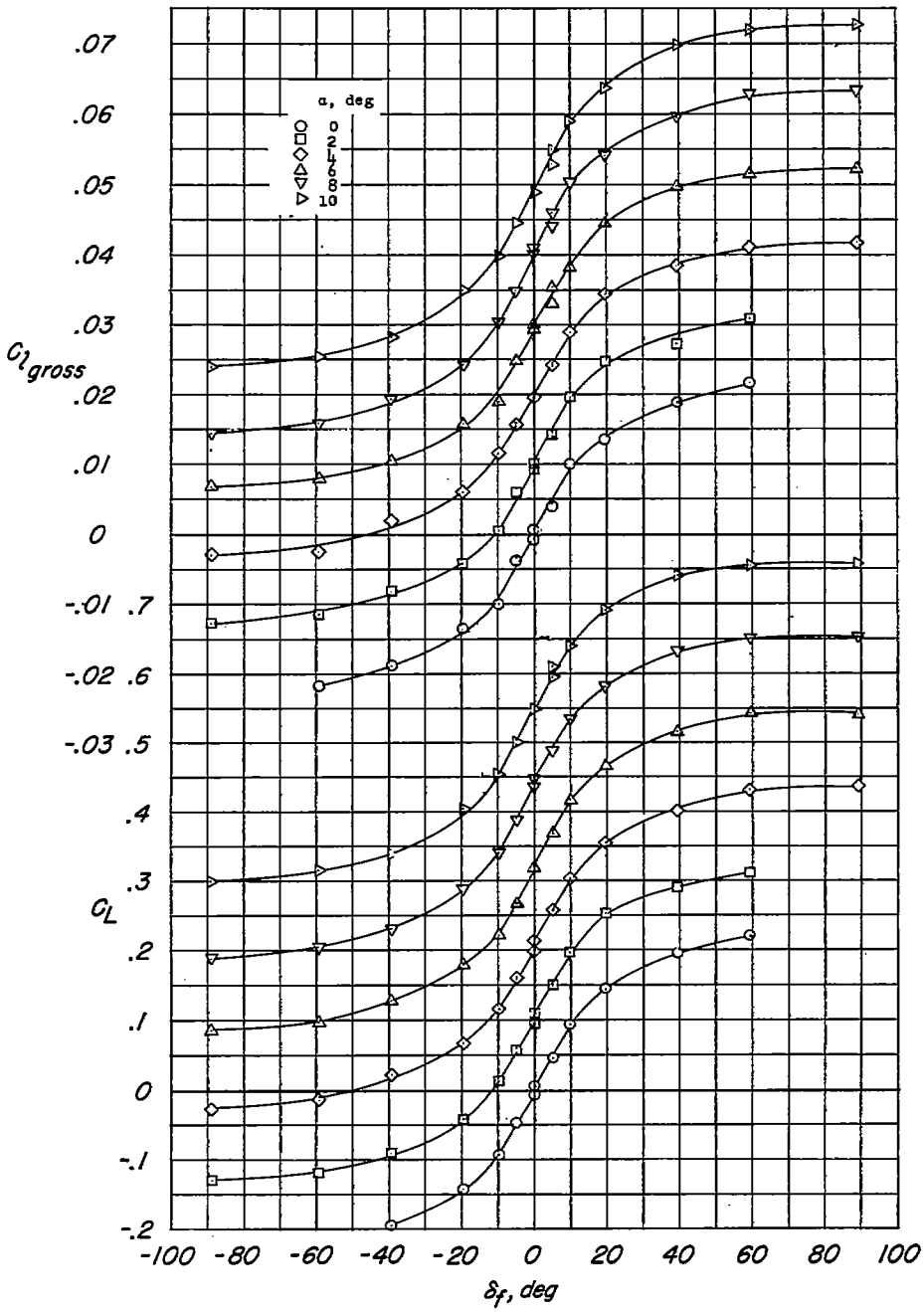

(a) M = 0.72.

Figure 3.- The variation with control deflection of gross rolling-moment coefficient and lift coefficient at various angles of attack.

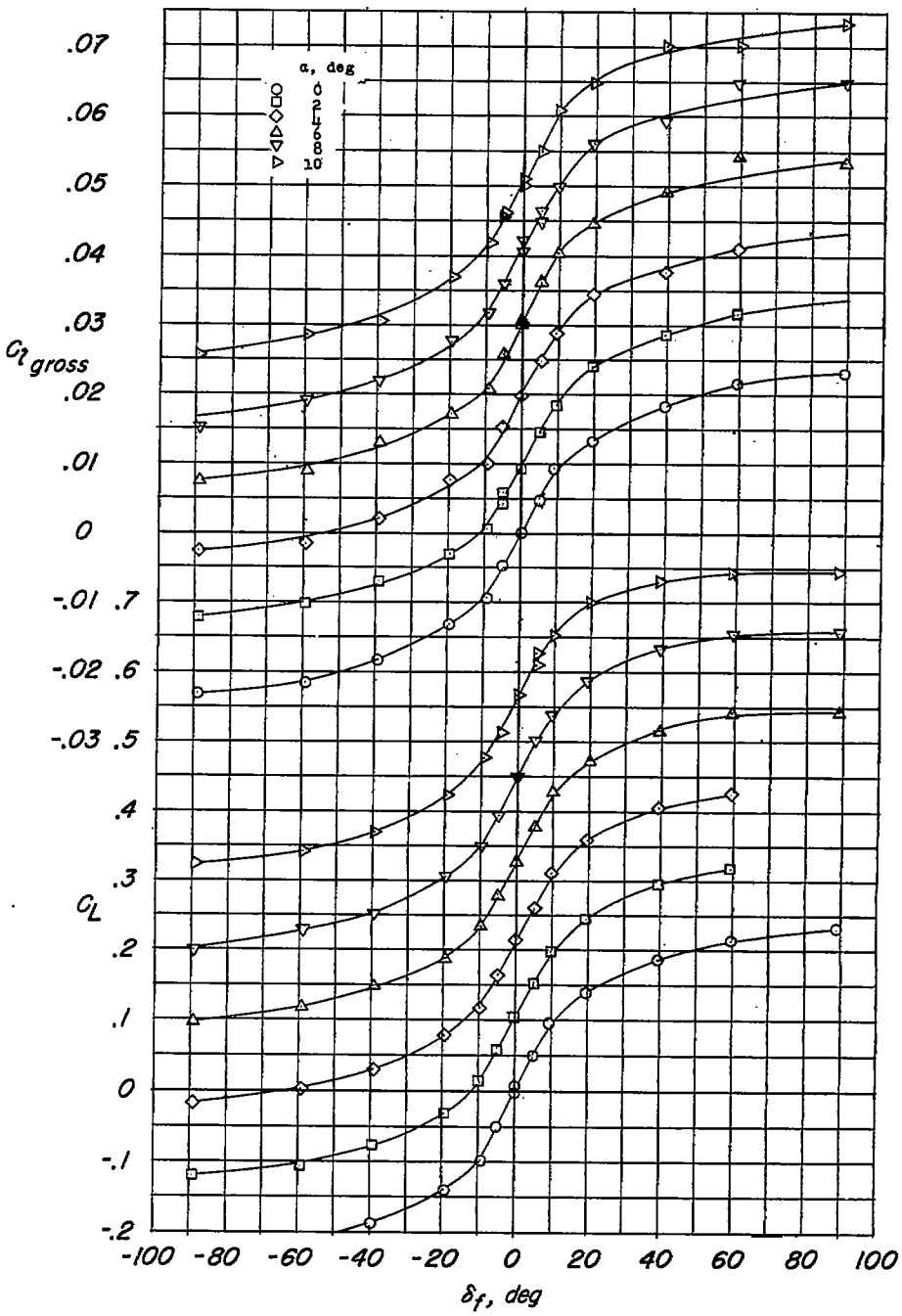

(b) M = 0.79.

Figure 3.- Continued.

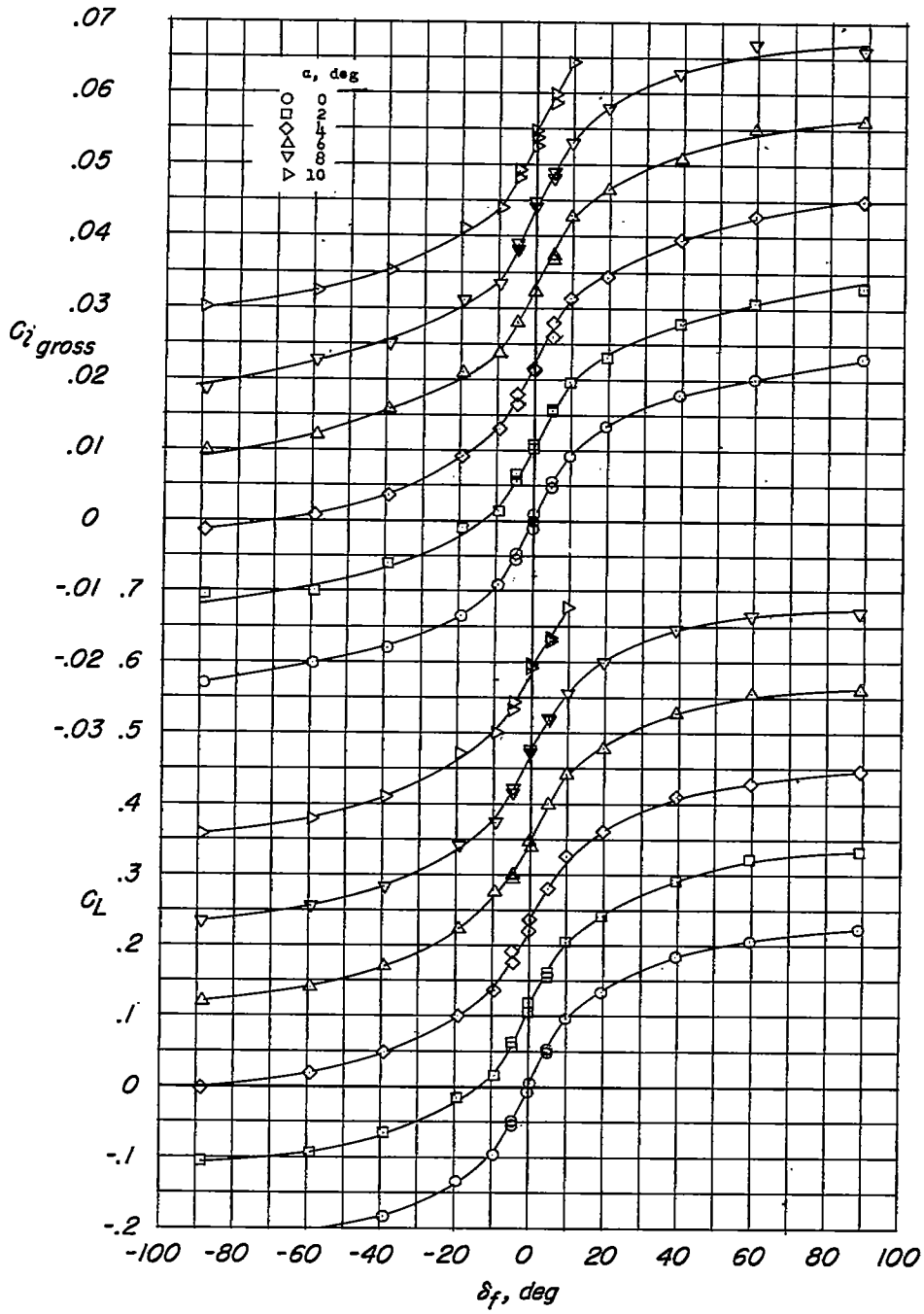

(c) M = 0.90.

Figure 3.- Continued.

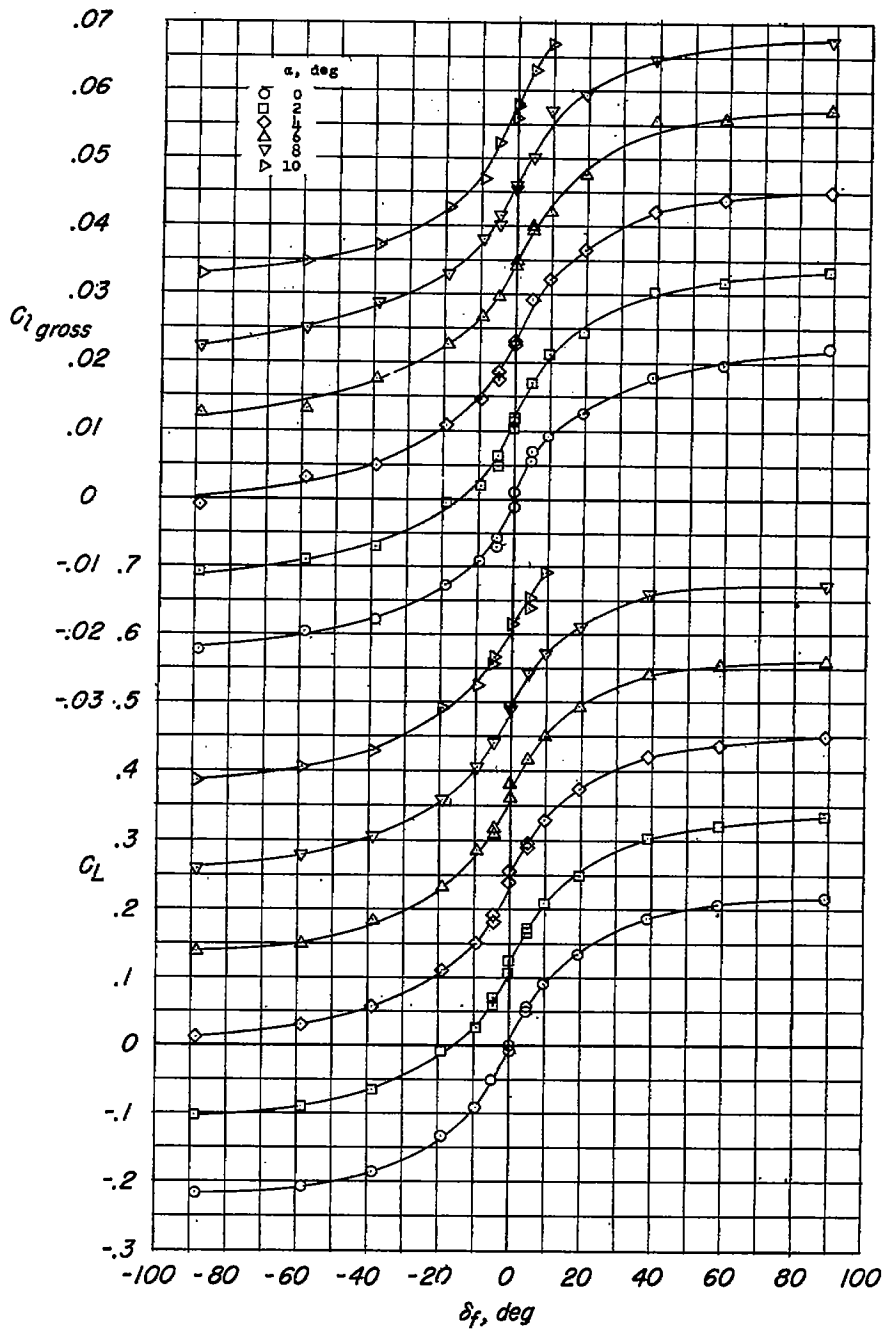

(d) M = 0.94.

Figure 3.- Continued.

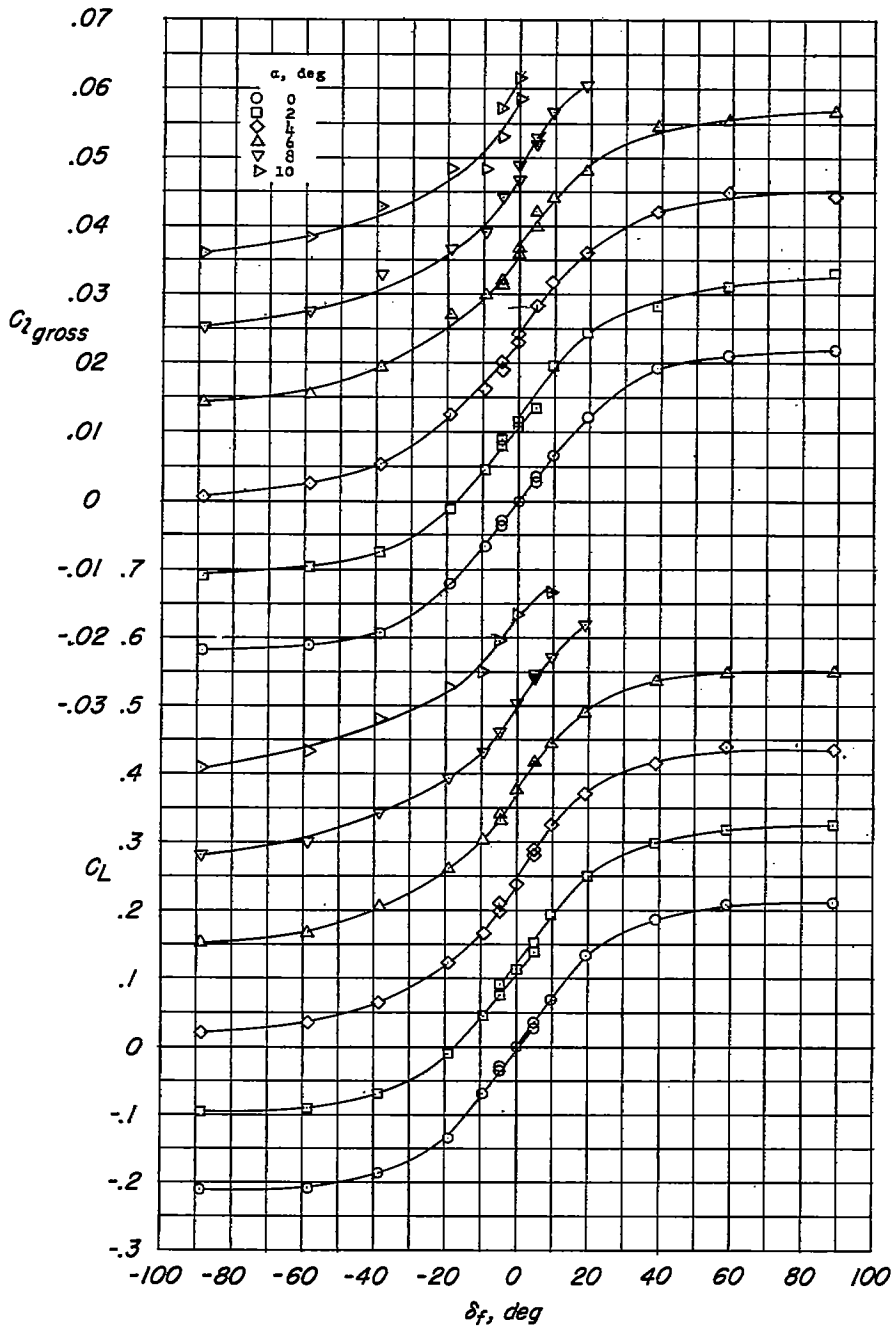

(e) M = 0.99.

Figure 3.- Continued.

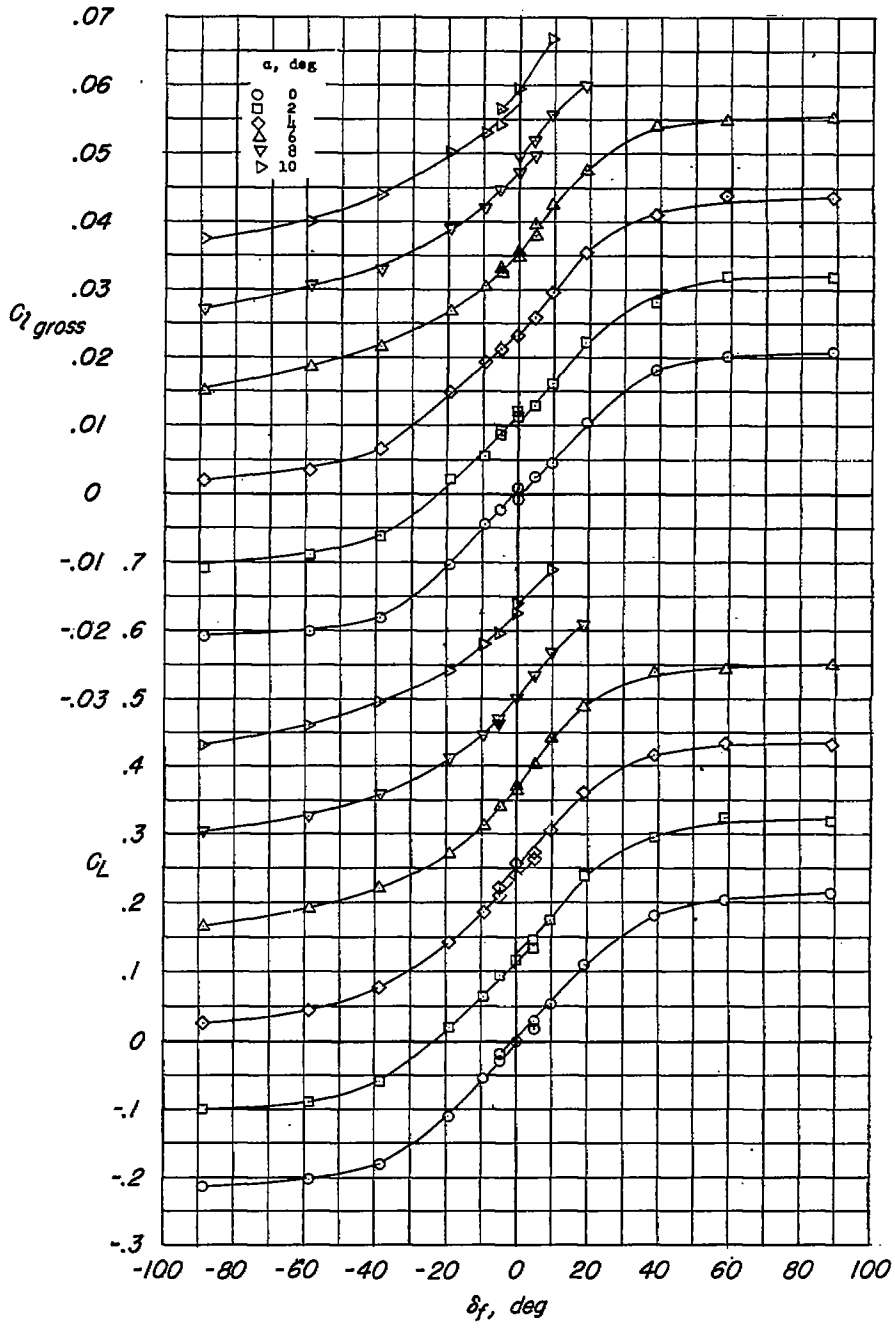

(f) M = 1.04.

Figure 3.- Continued.

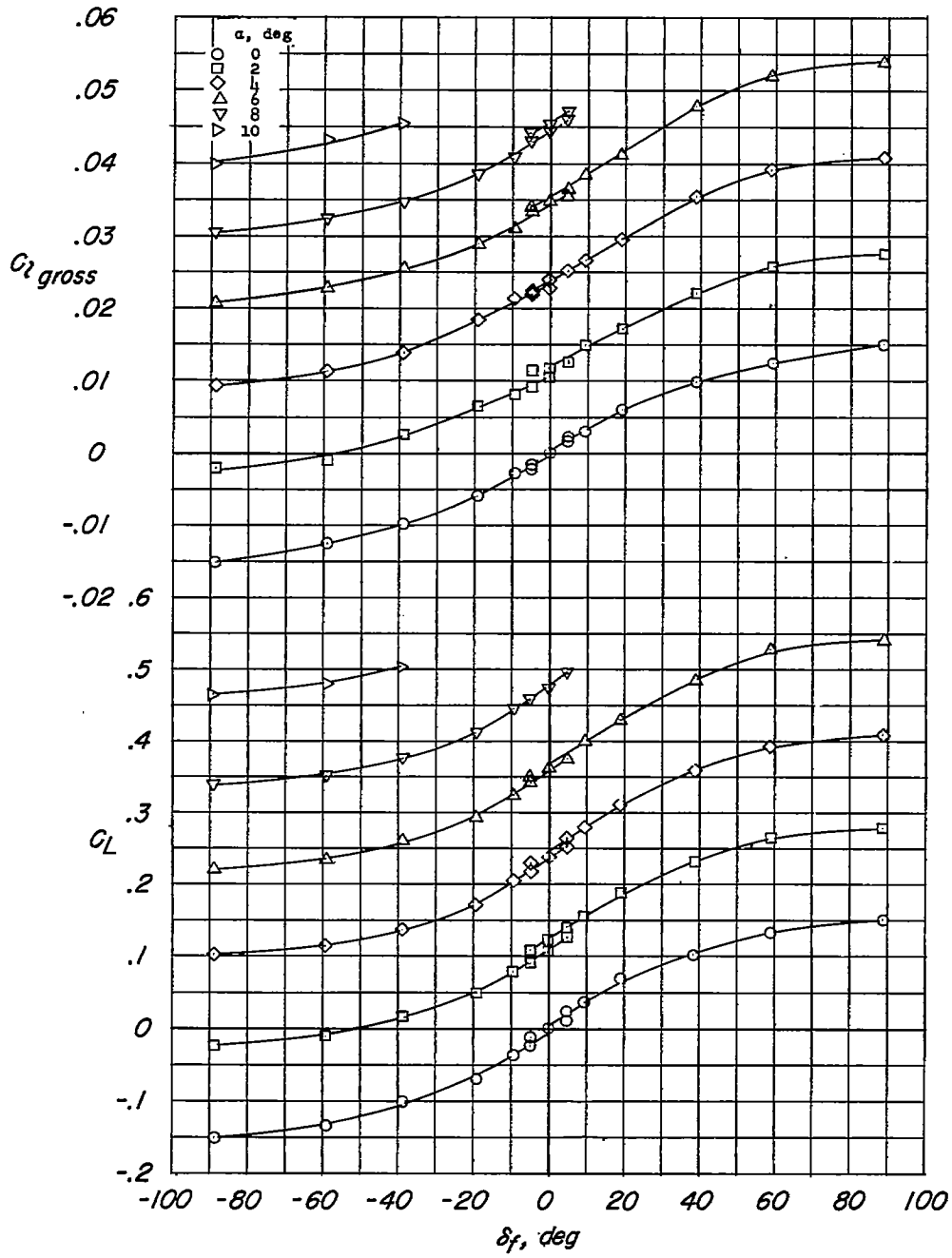

(g) M = 1.20.

Figure 3.- Continued.

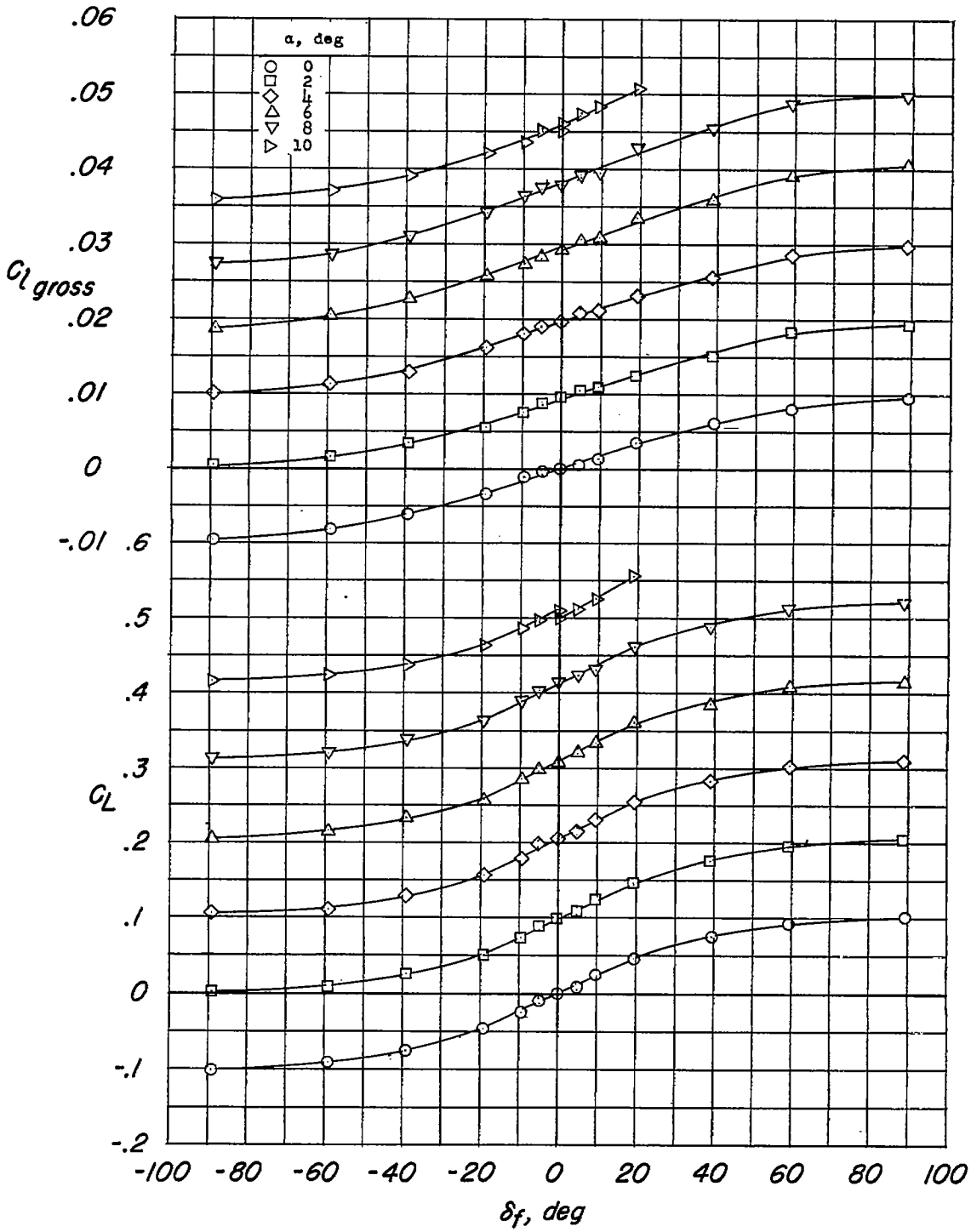

(h) M = 1.41.

Figure 3.- Continued.

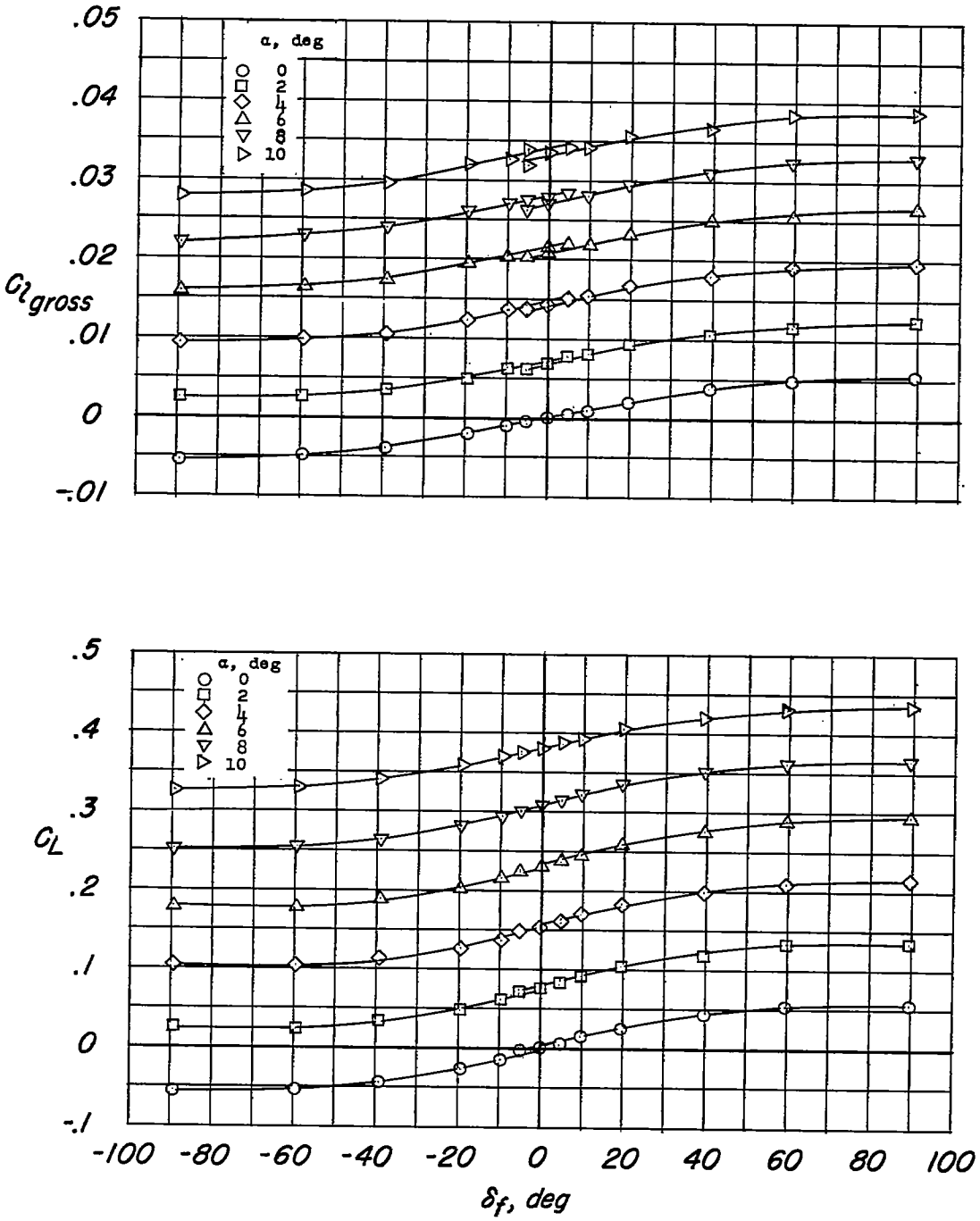

(i) M = 1.96.

Figure 3.- Concluded.

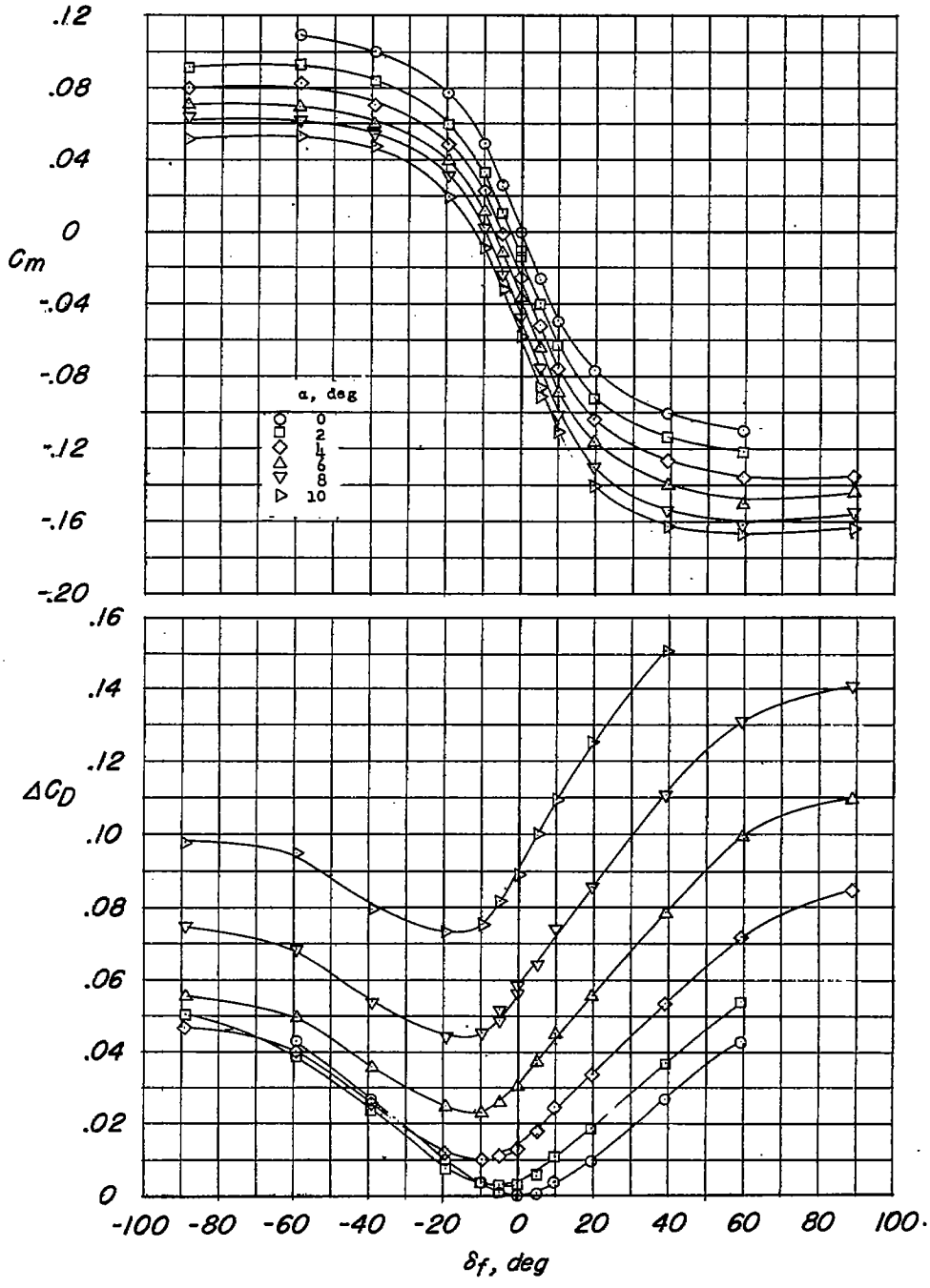

(a) M = 0.72.

Figure 4.- Variation with control deflection of pitching-moment and incremental drag coefficients at various angles of attack.

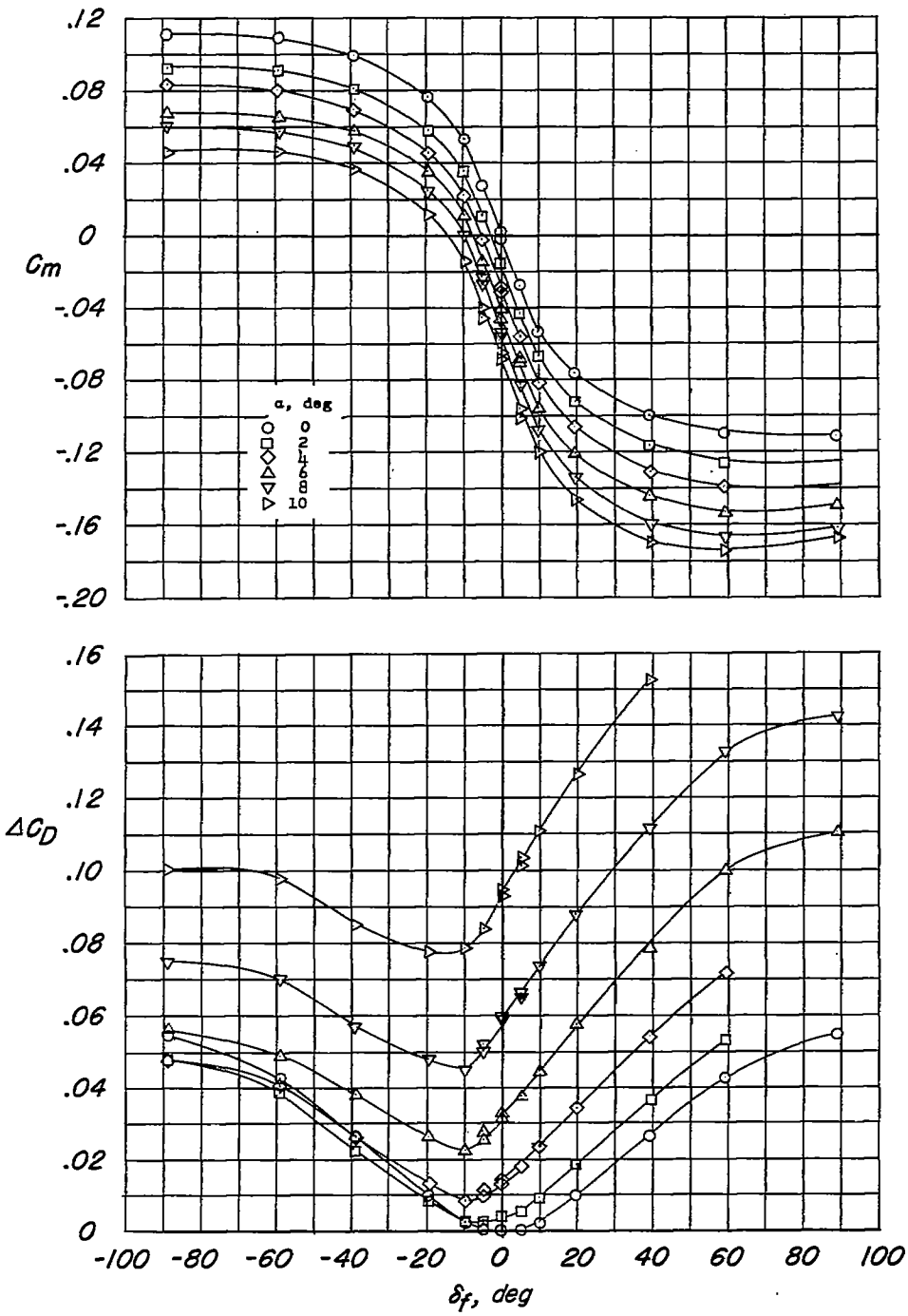

(b) M = 0.79.

Figure 4.- Continued.

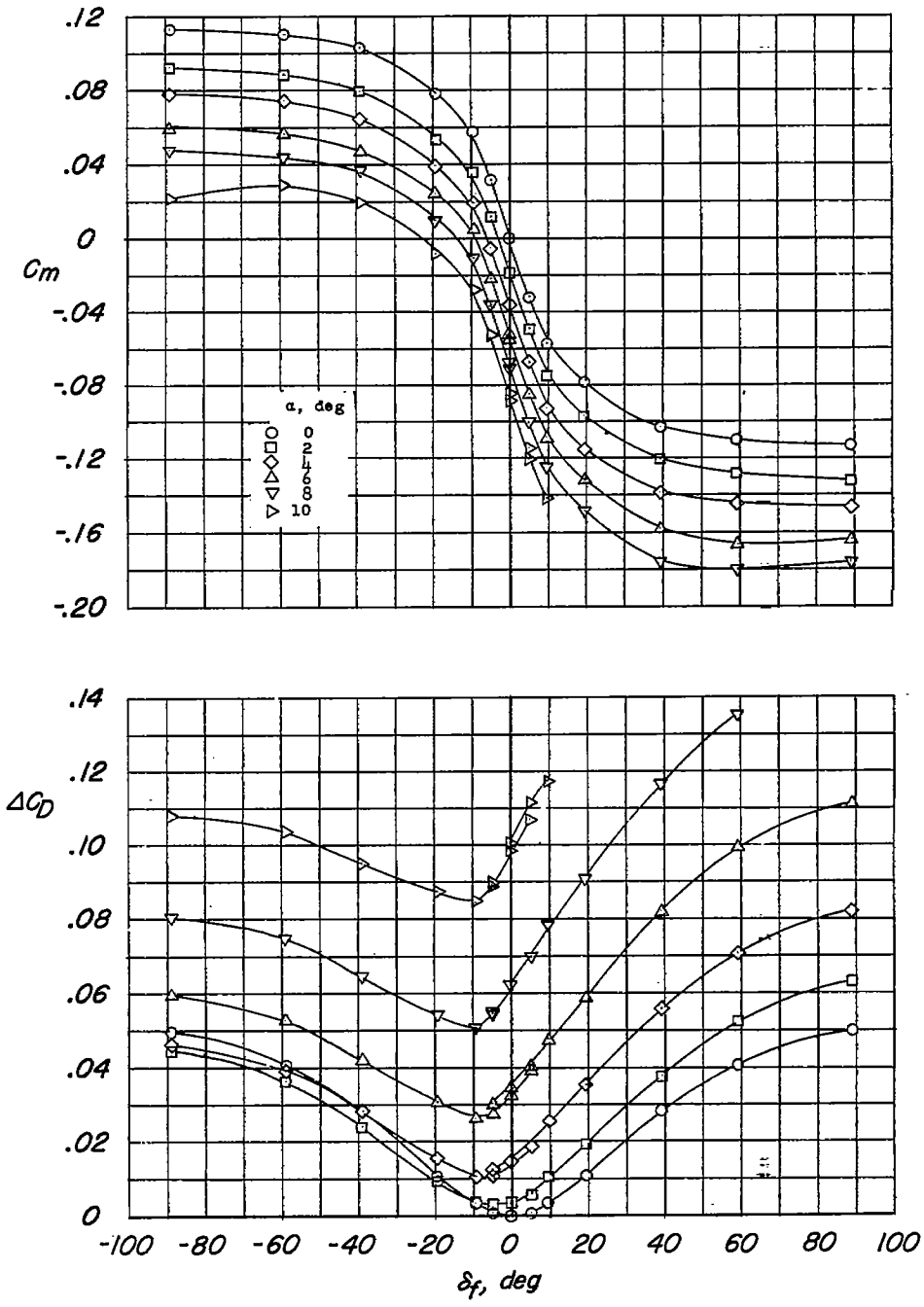

(c) M = 0.90.

Figure 4.- Continued.

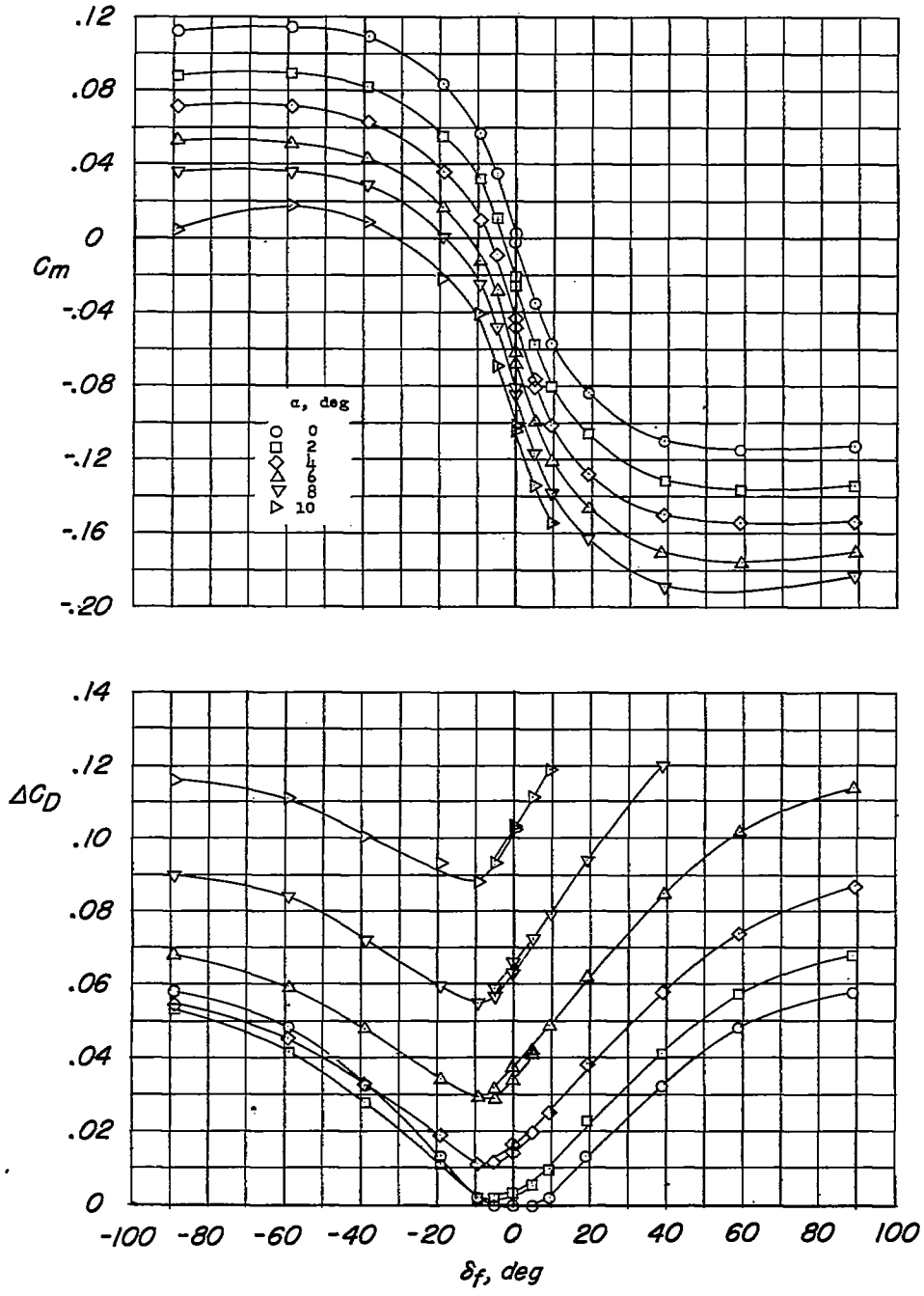

(d) M = 0.94.

Figure 4.- Continued.

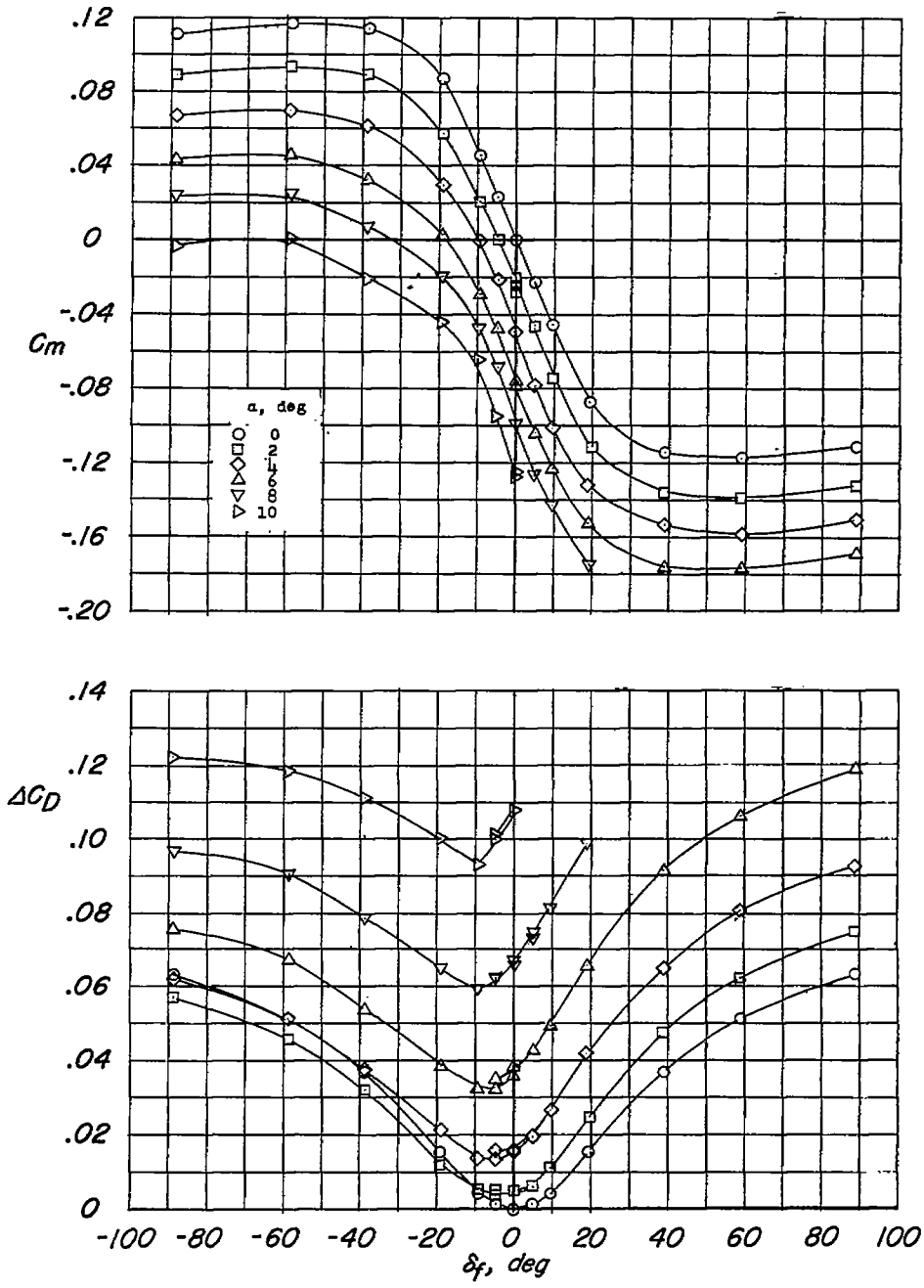

(e) M = 0.99.

Figure 4.- Continued.

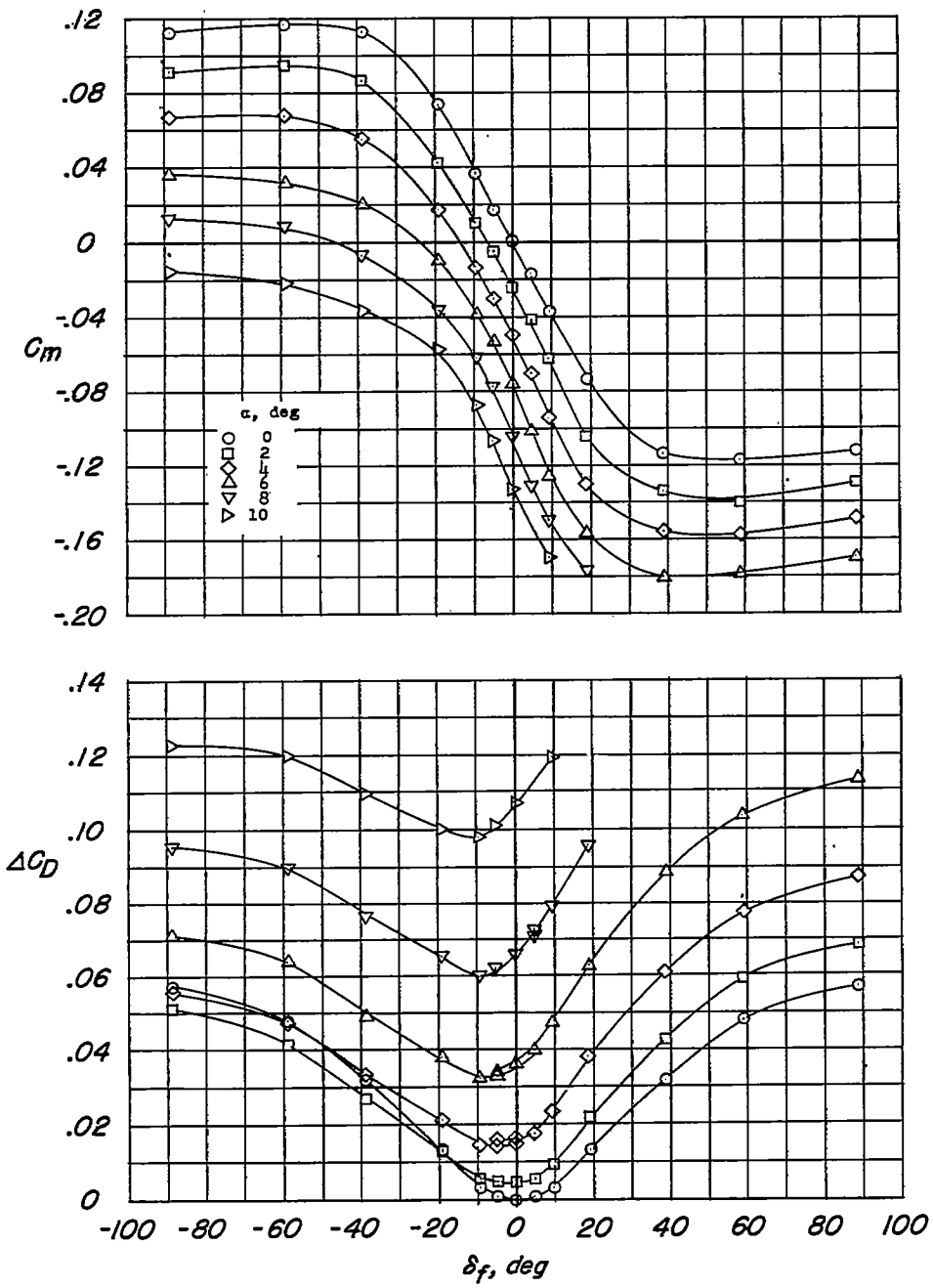

(f) M = 1.04.

Figure 4.- Continued.

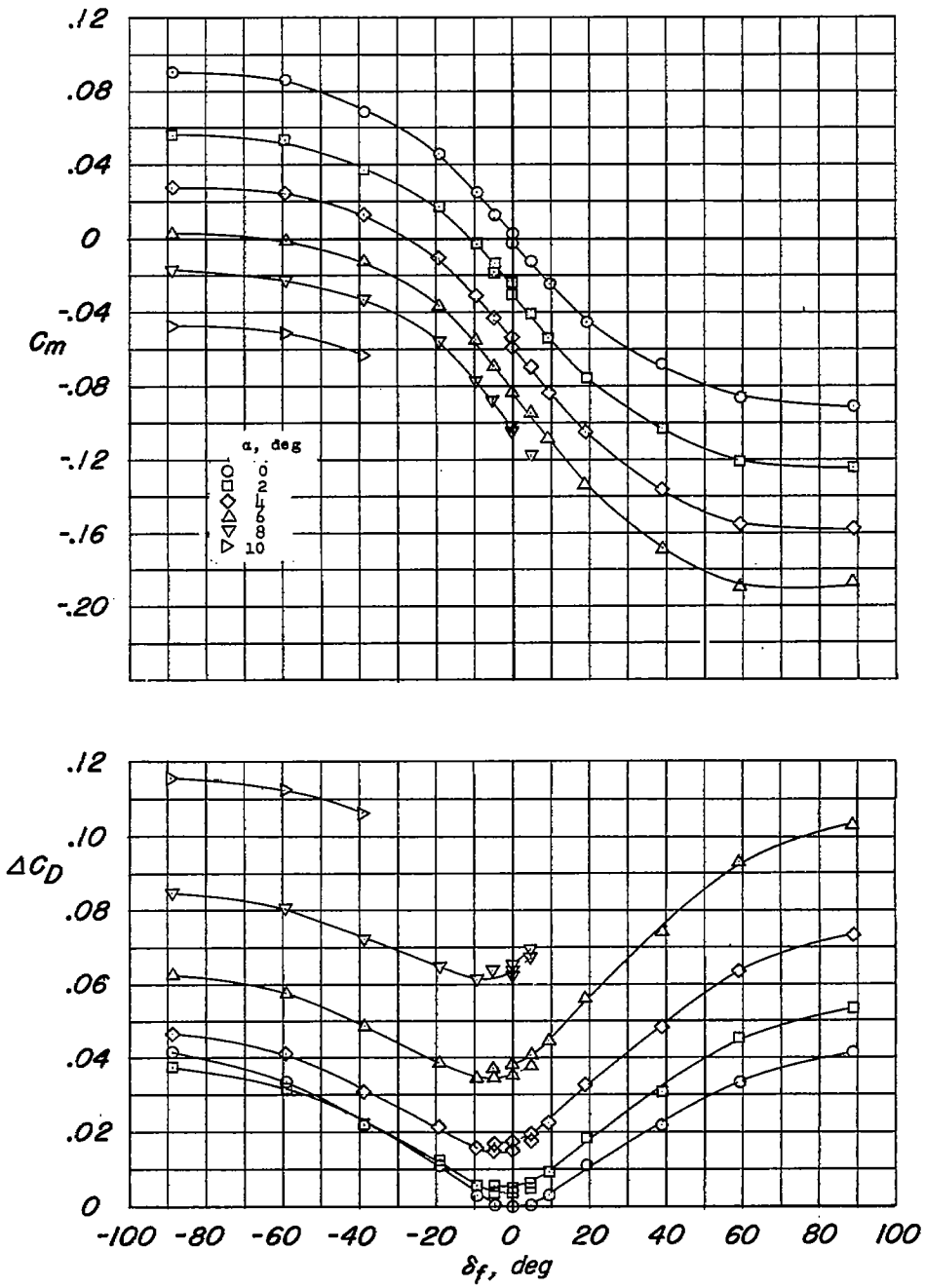

(g) M = 1.20.

Figure 4.- Continued.

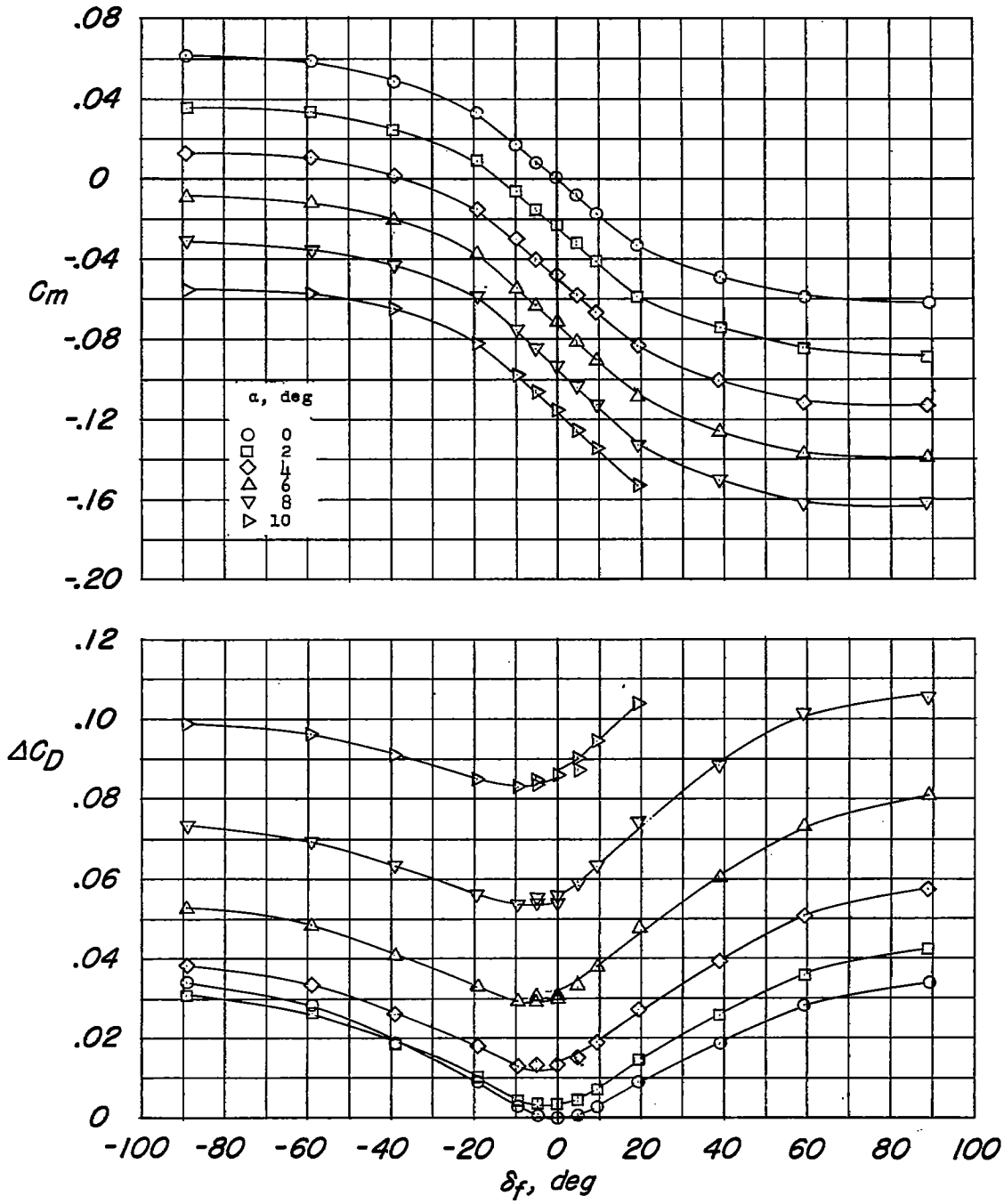

(h) M = 1.41.

Figure 4.- Continued.

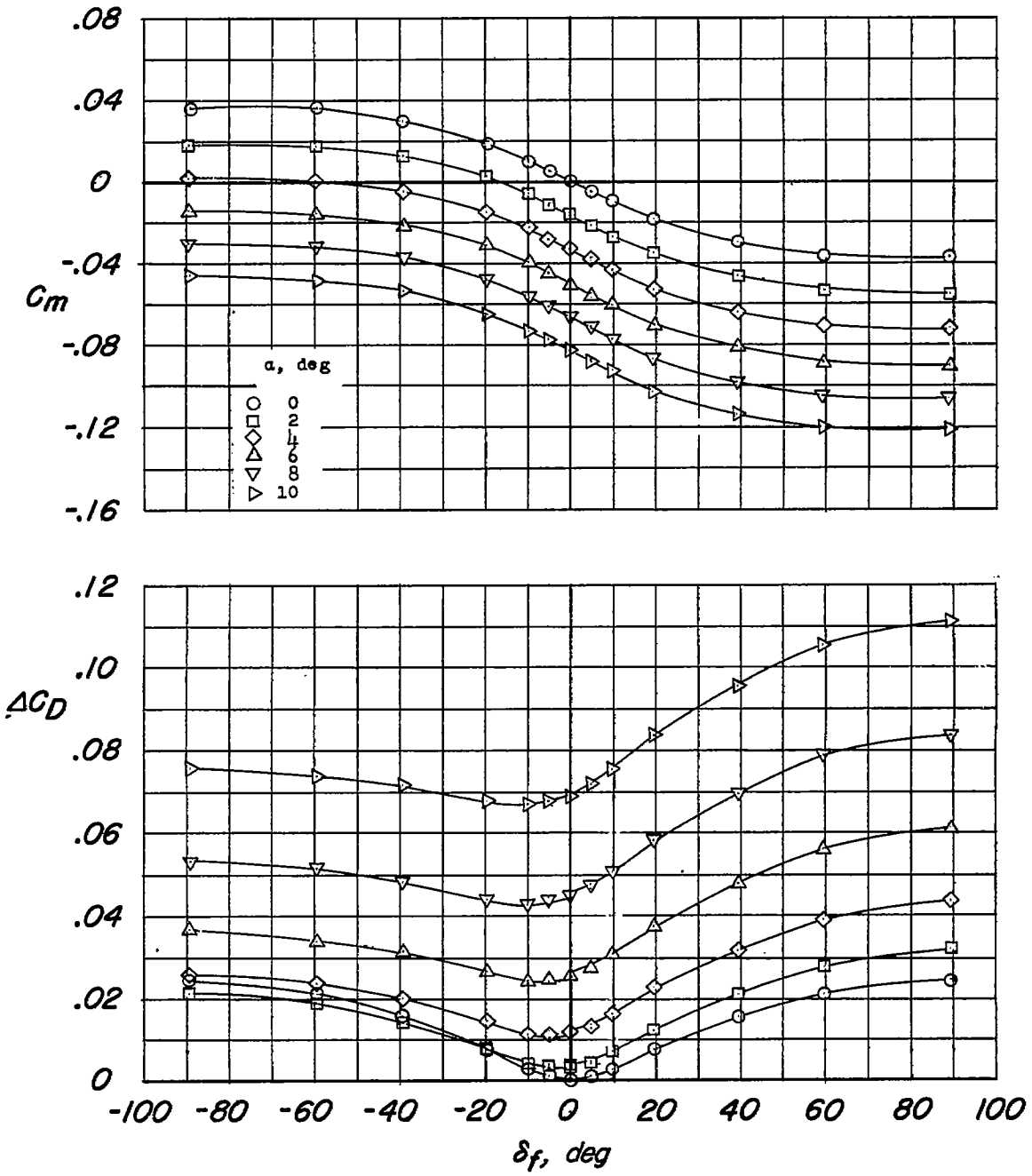

(i) M = 1.96.

Figure 4.- Concluded.

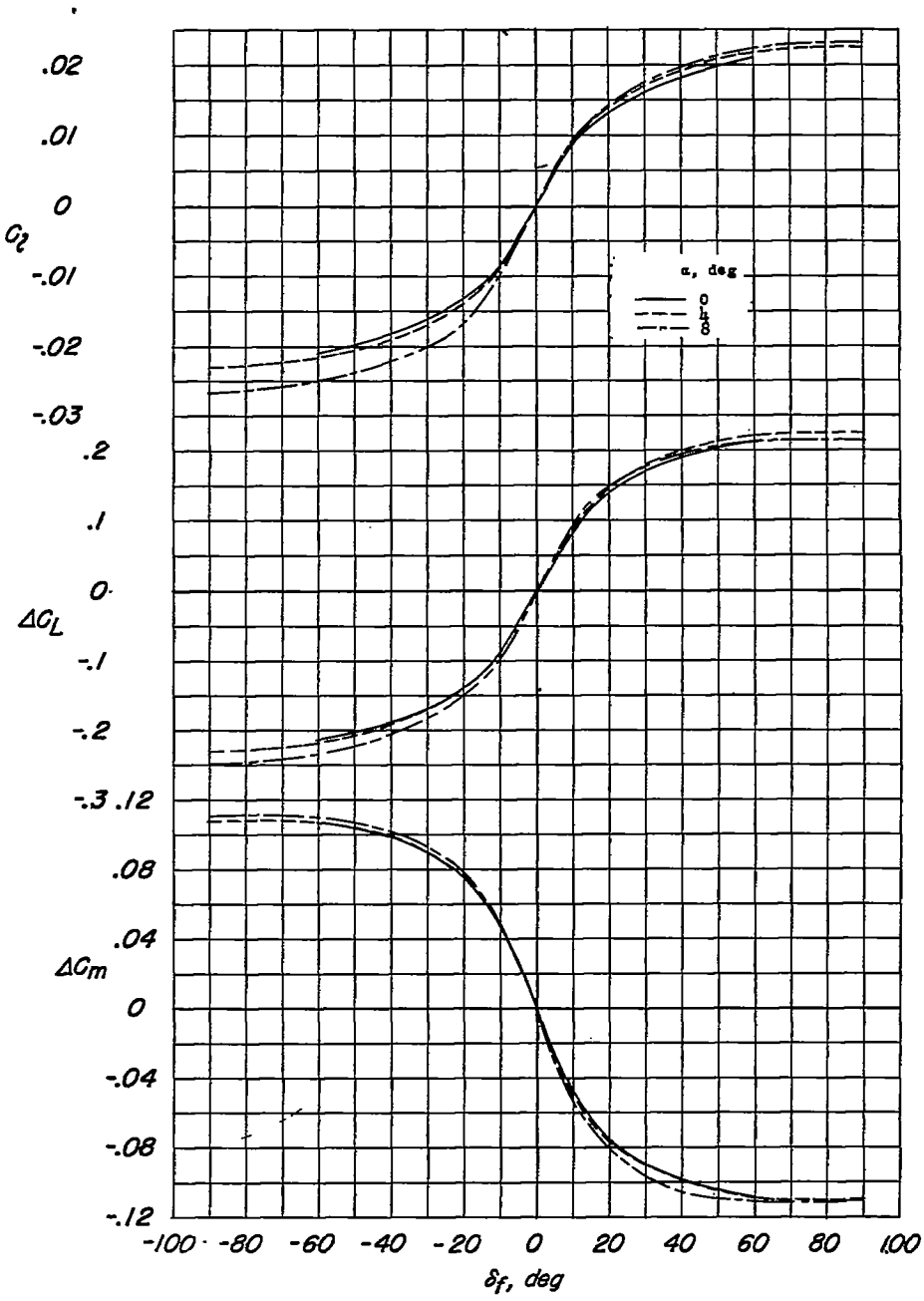

(a) M = 0.72.

Figure 5.- The variation with control deflection of rolling-moment coefficient and increments of lift and pitching-moment coefficients due to control deflection at various angles of attack.

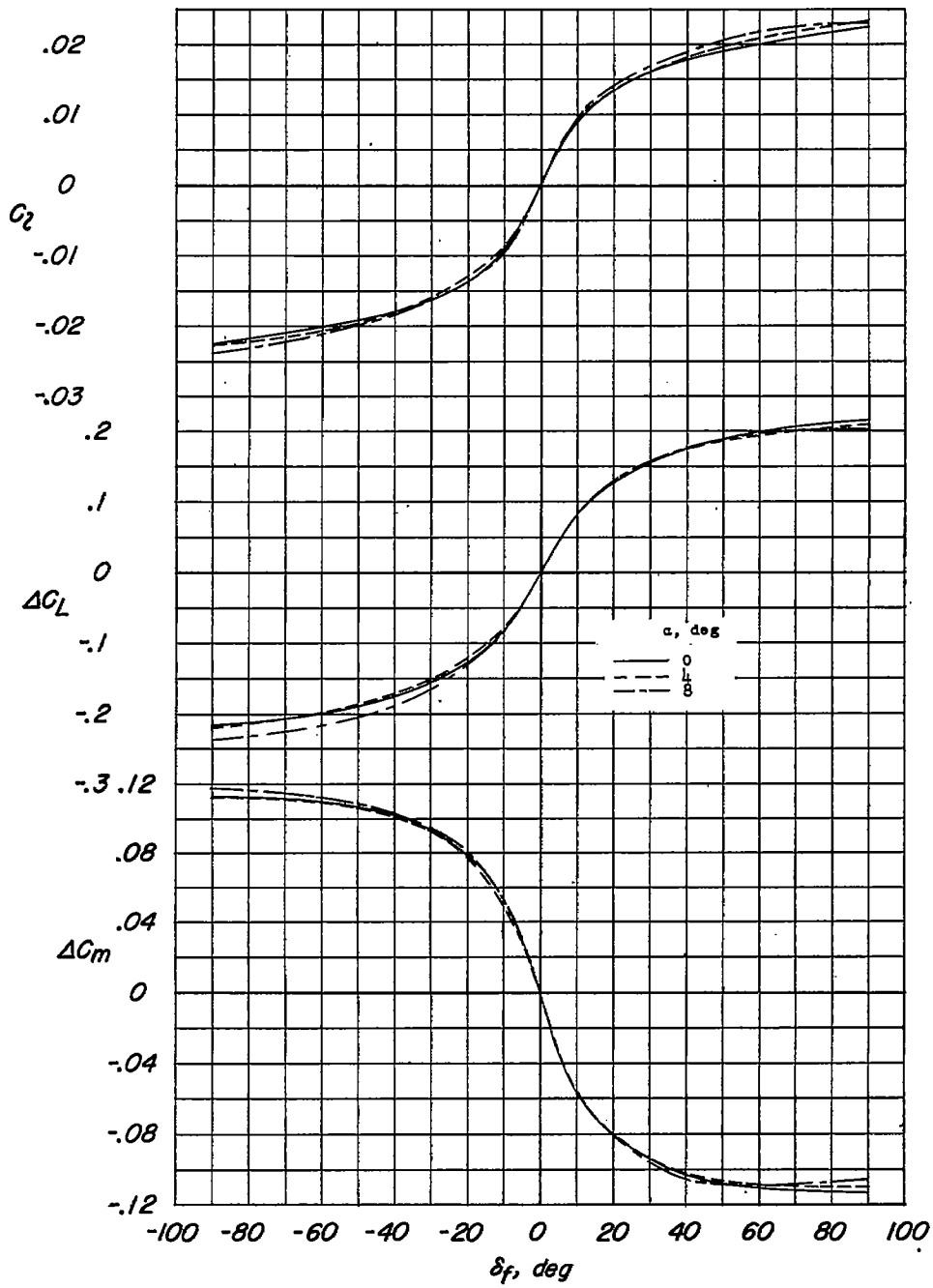

(b) M = 0.90.

Figure 5.- Continued.

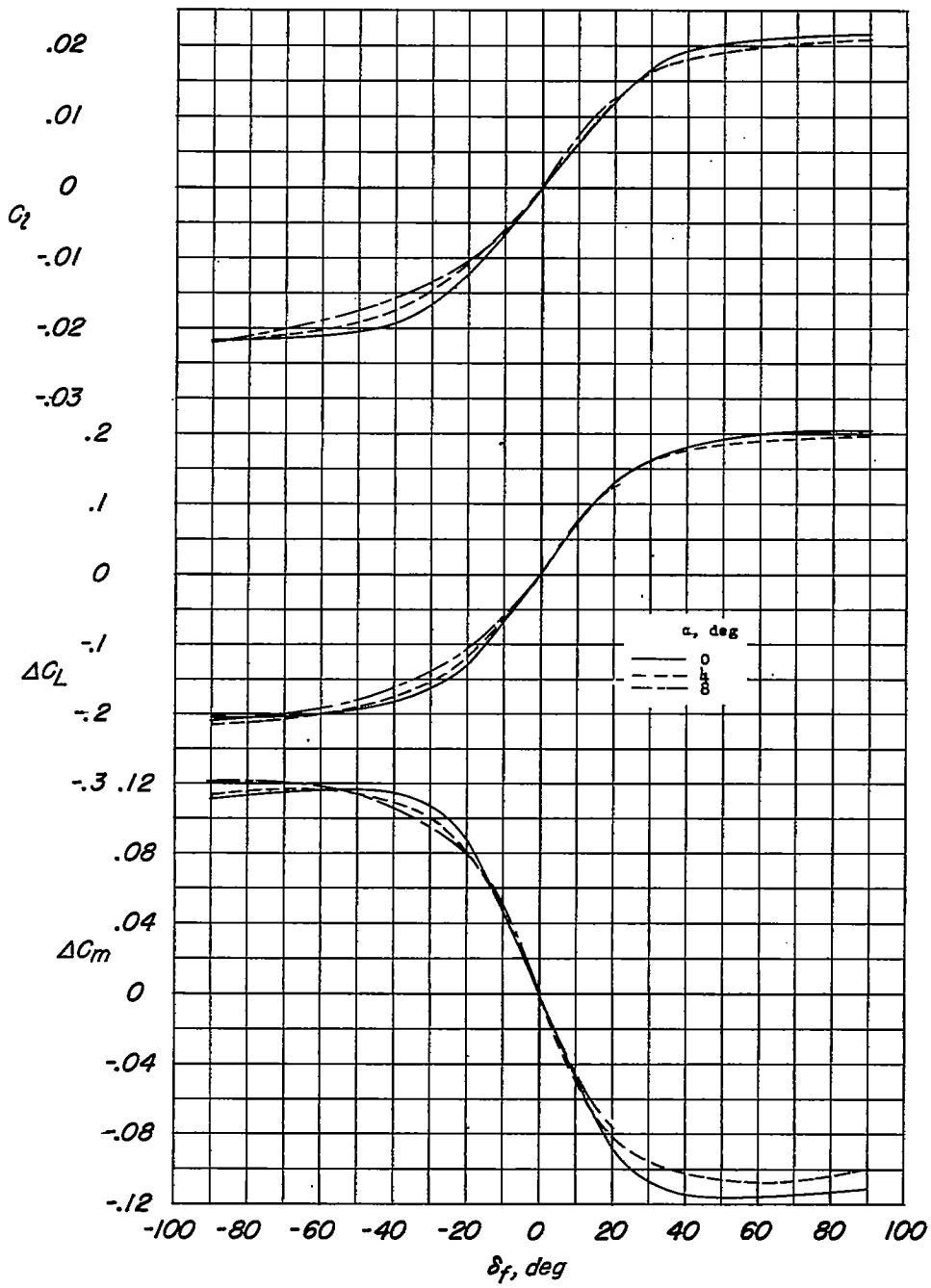

(c) M = 0.99.

Figure 5.- Continued.

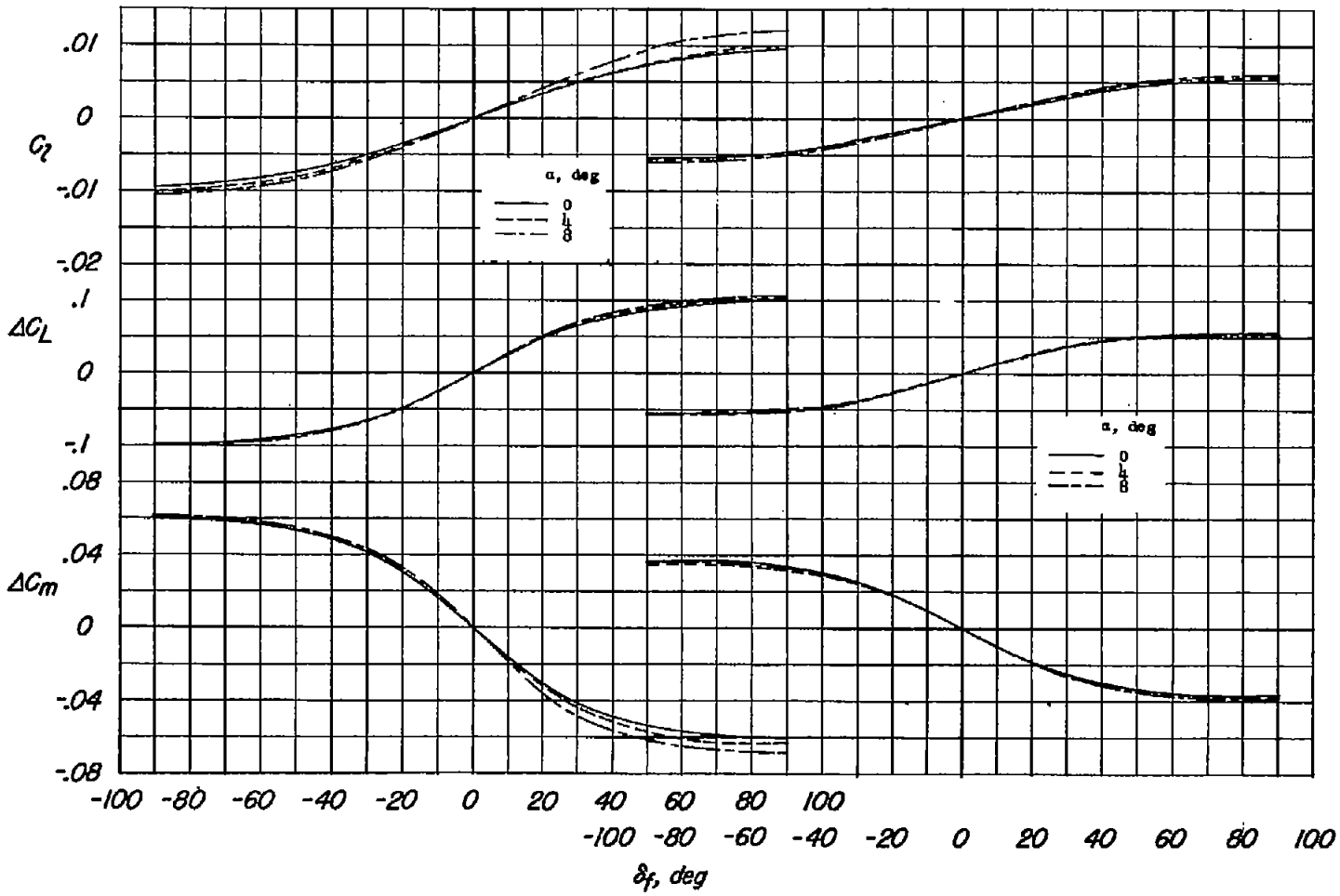

(d) M = 1.41.

(e) M = 1.96.

Figure 5.- Concluded.

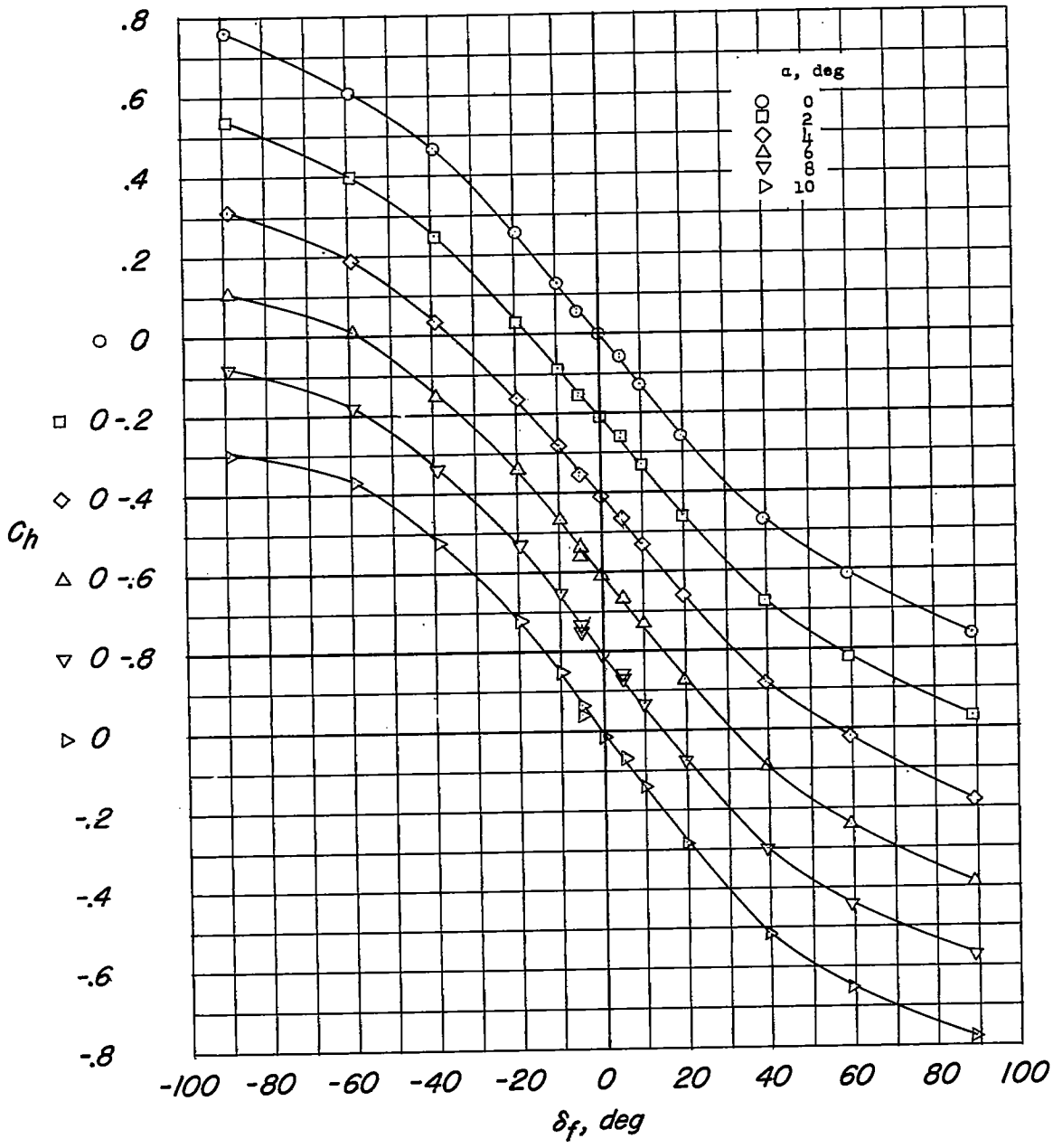

(a) M = 0.72.

Figure 6.- Variation of hinge-moment coefficient with control deflection at various angles of attack.

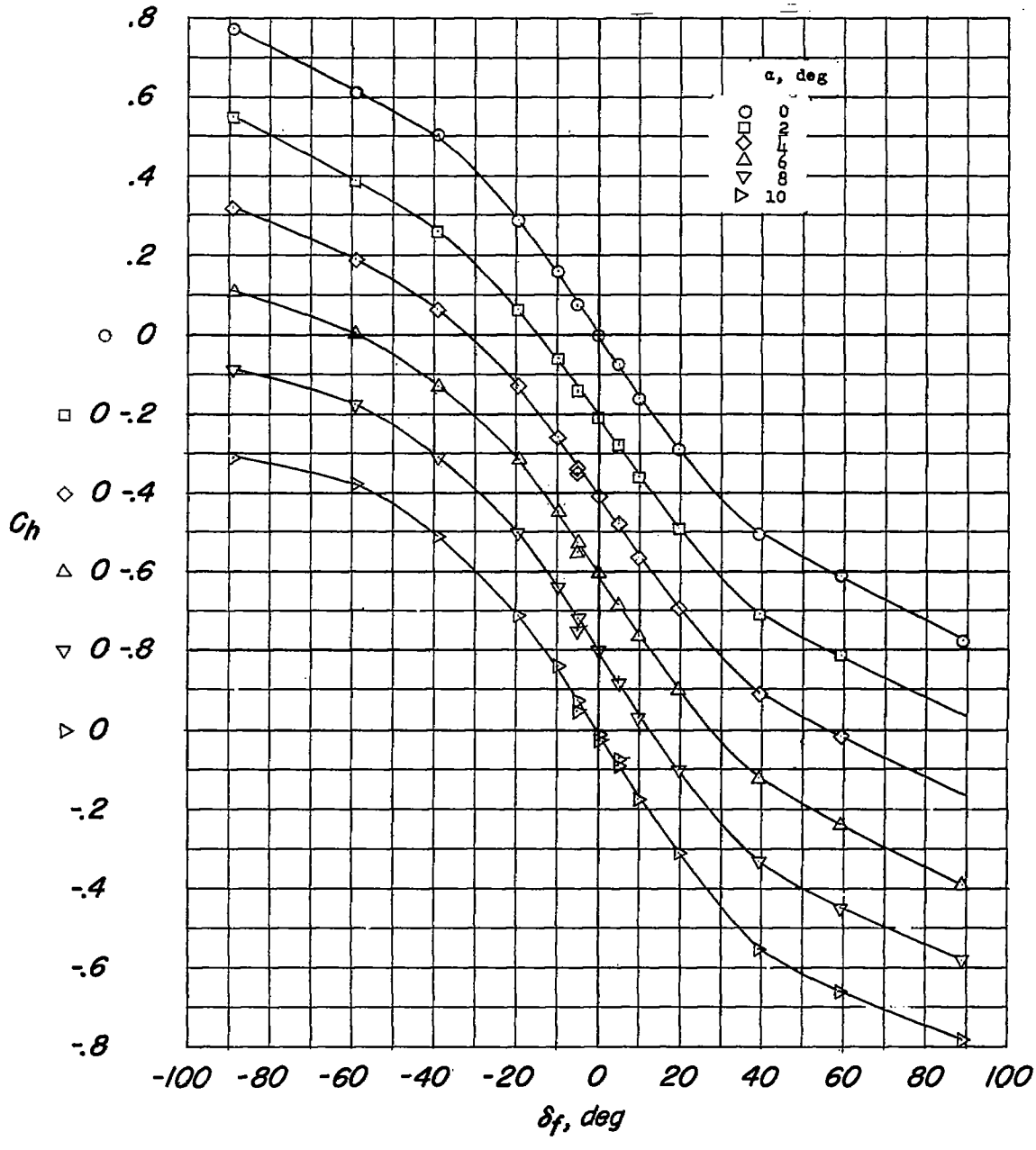

(b) M = 0.79.

Figure 6.- Continued.

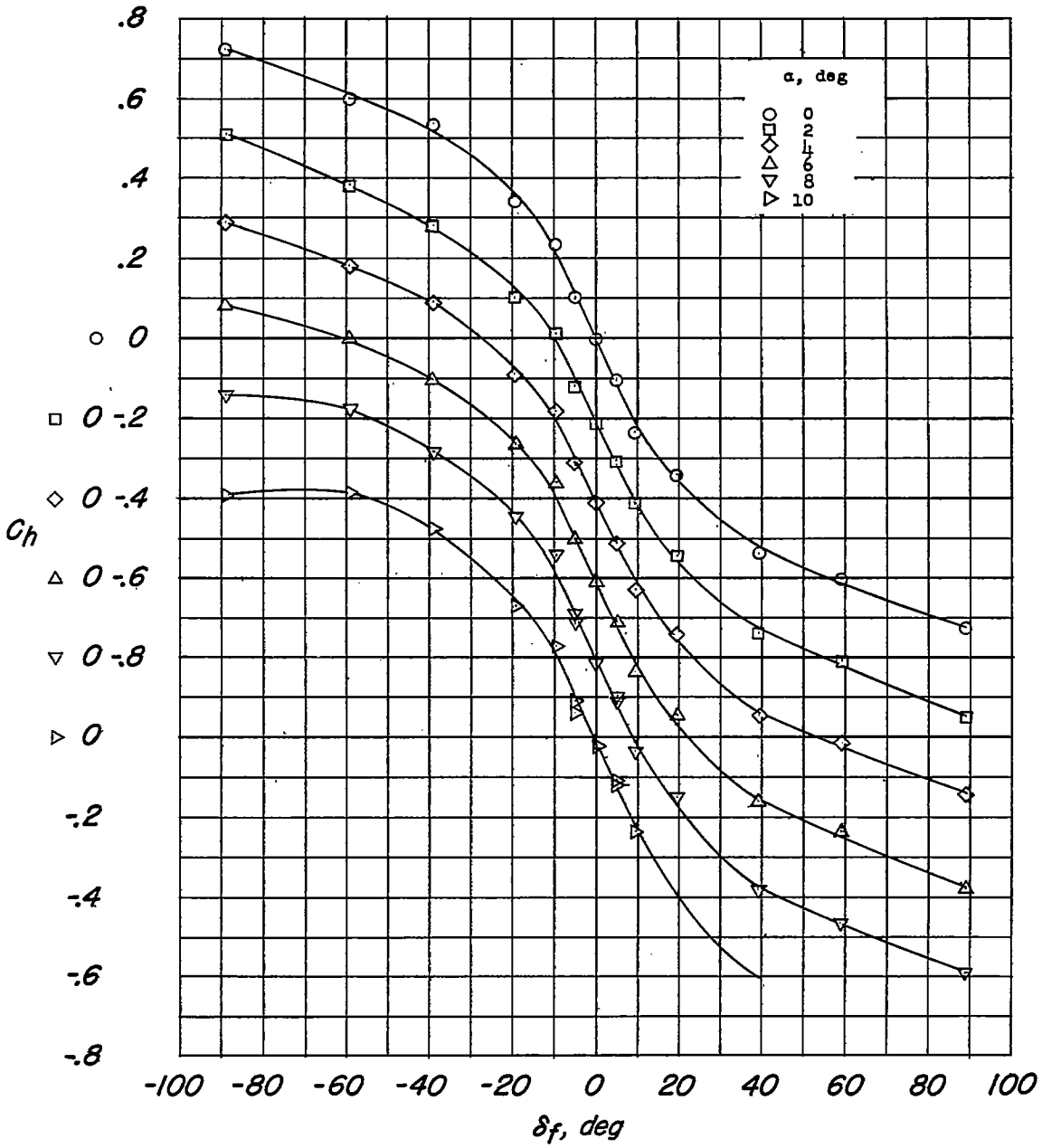

(c) M = 0.90.

Figure 6.- Continued.

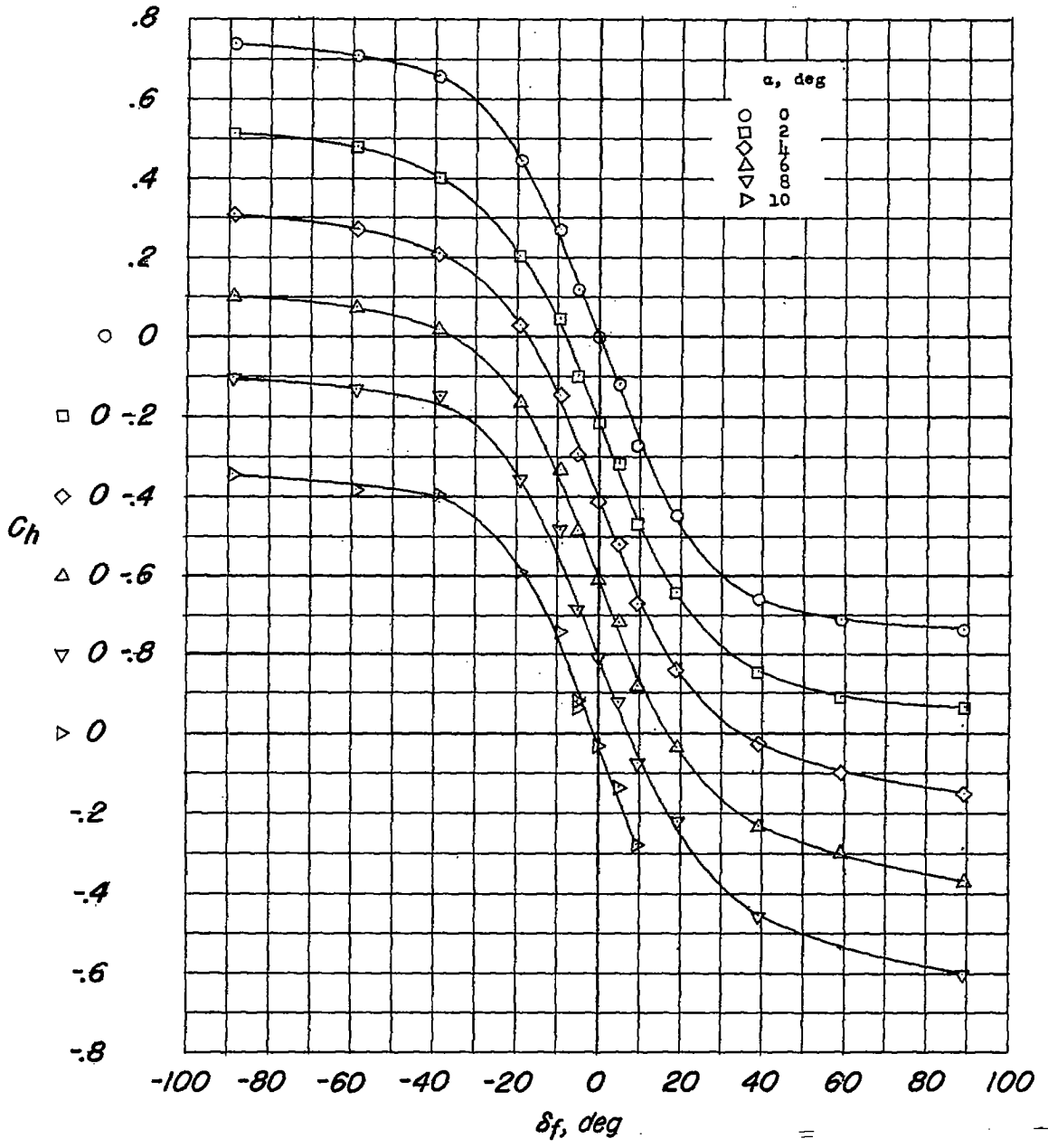

(d) M = 0.94.

Figure 6.- Continued.

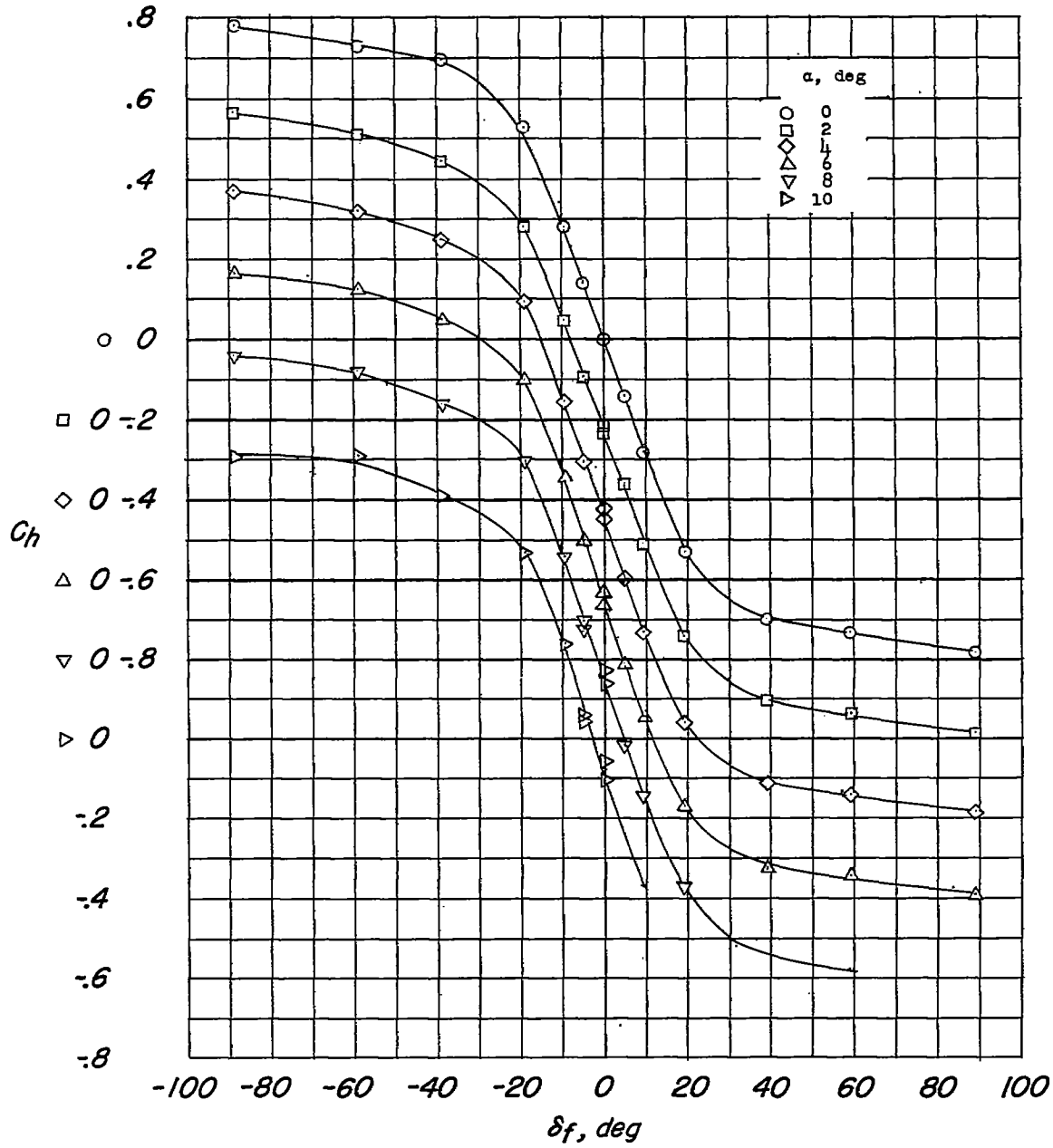

(e) M = 0.99.

Figure 6.- Continued.

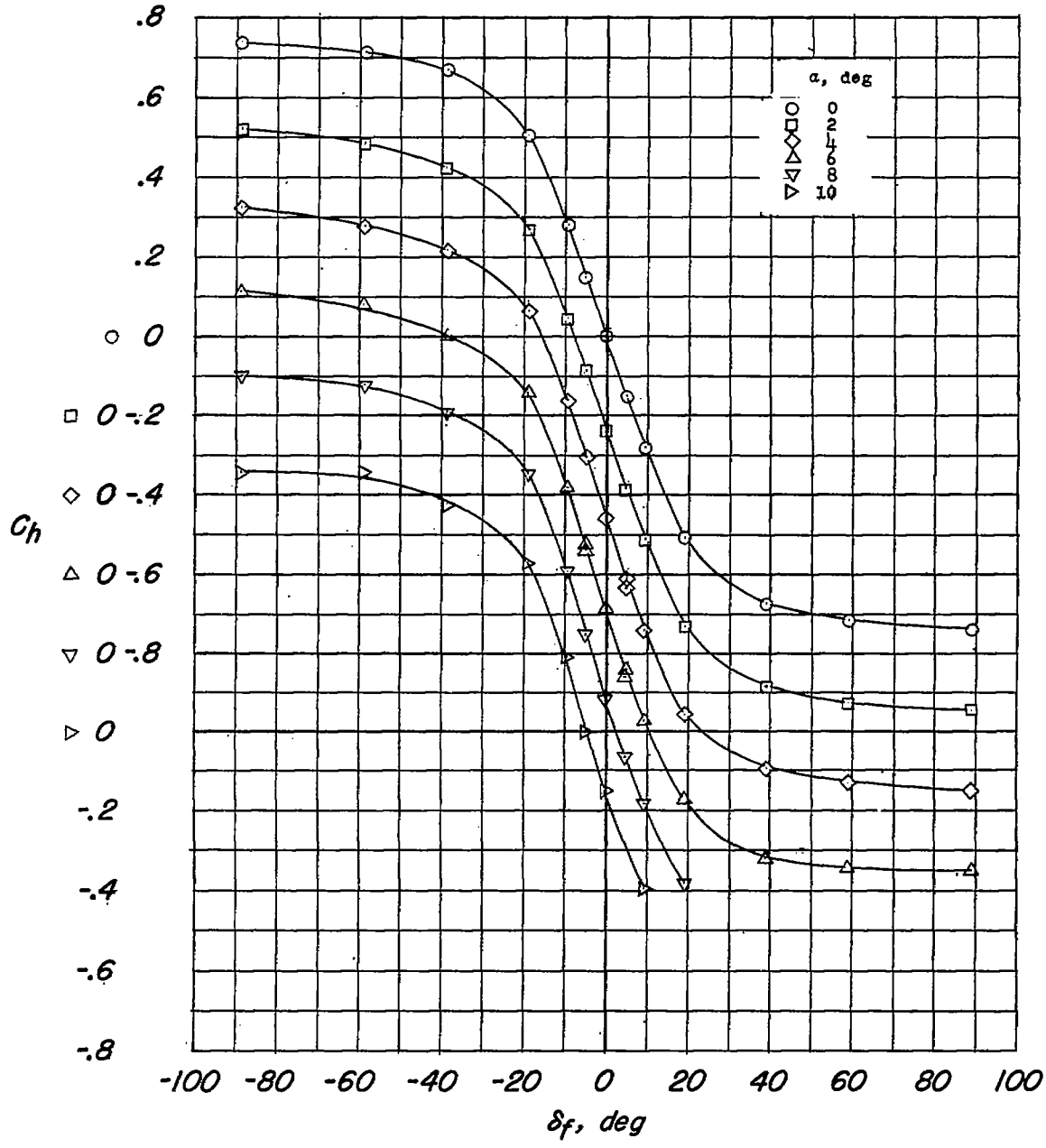

(f) M = 1.04.

Figure 6.- Continued.

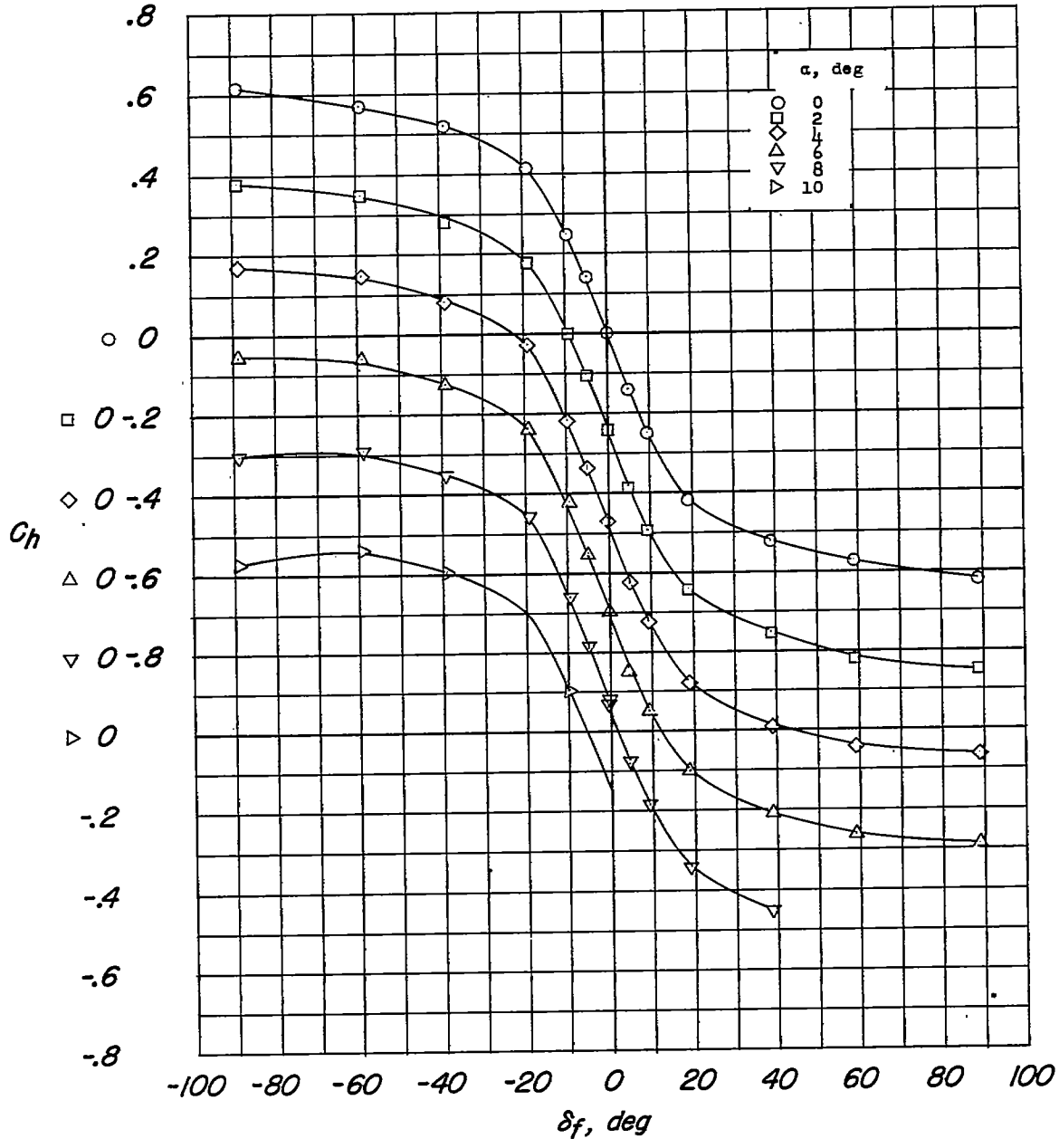

(g) M = 1.20.

Figure 6.- Continued.

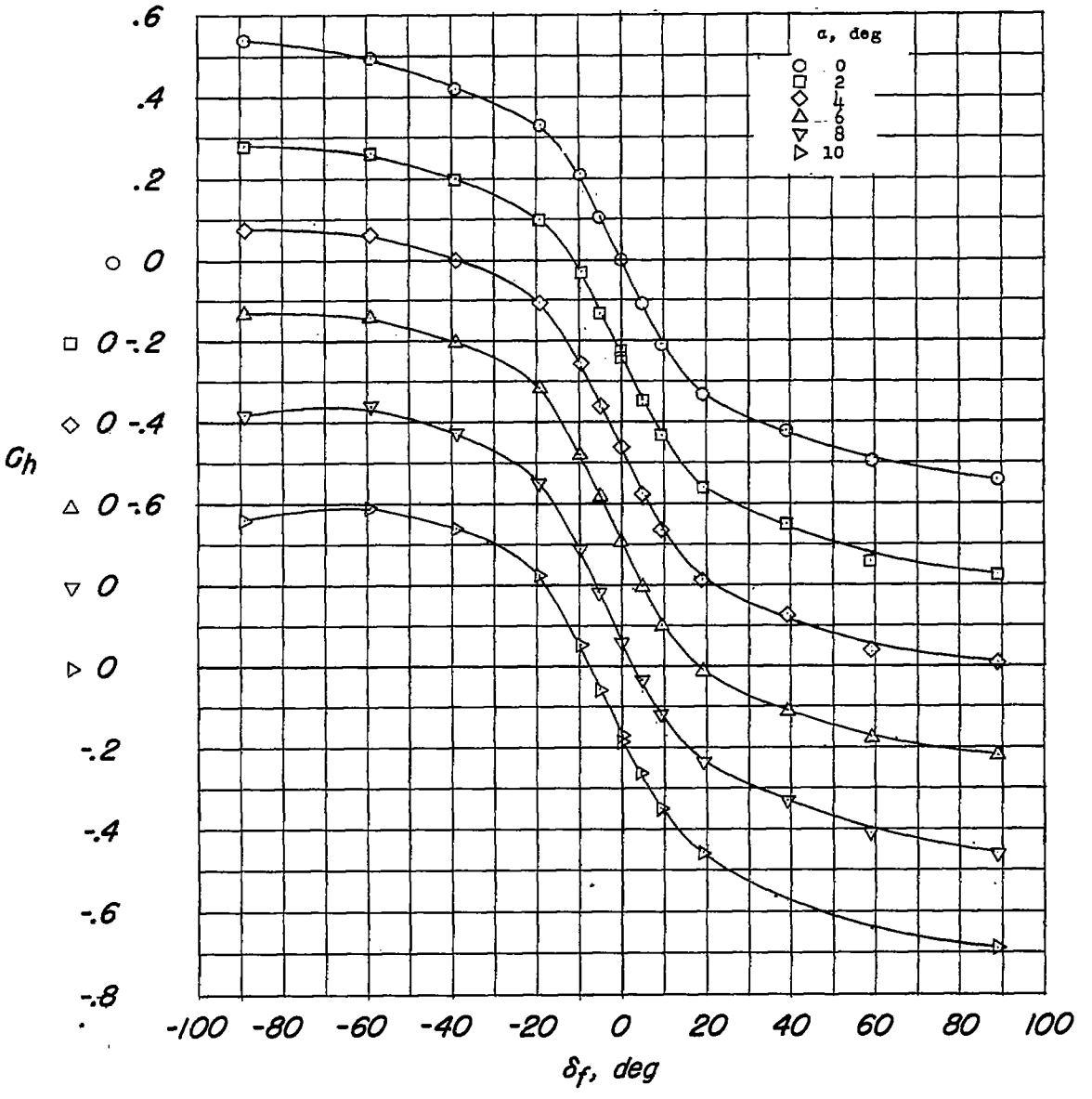

(h) M = 1.41.

Figure 6.- Continued.

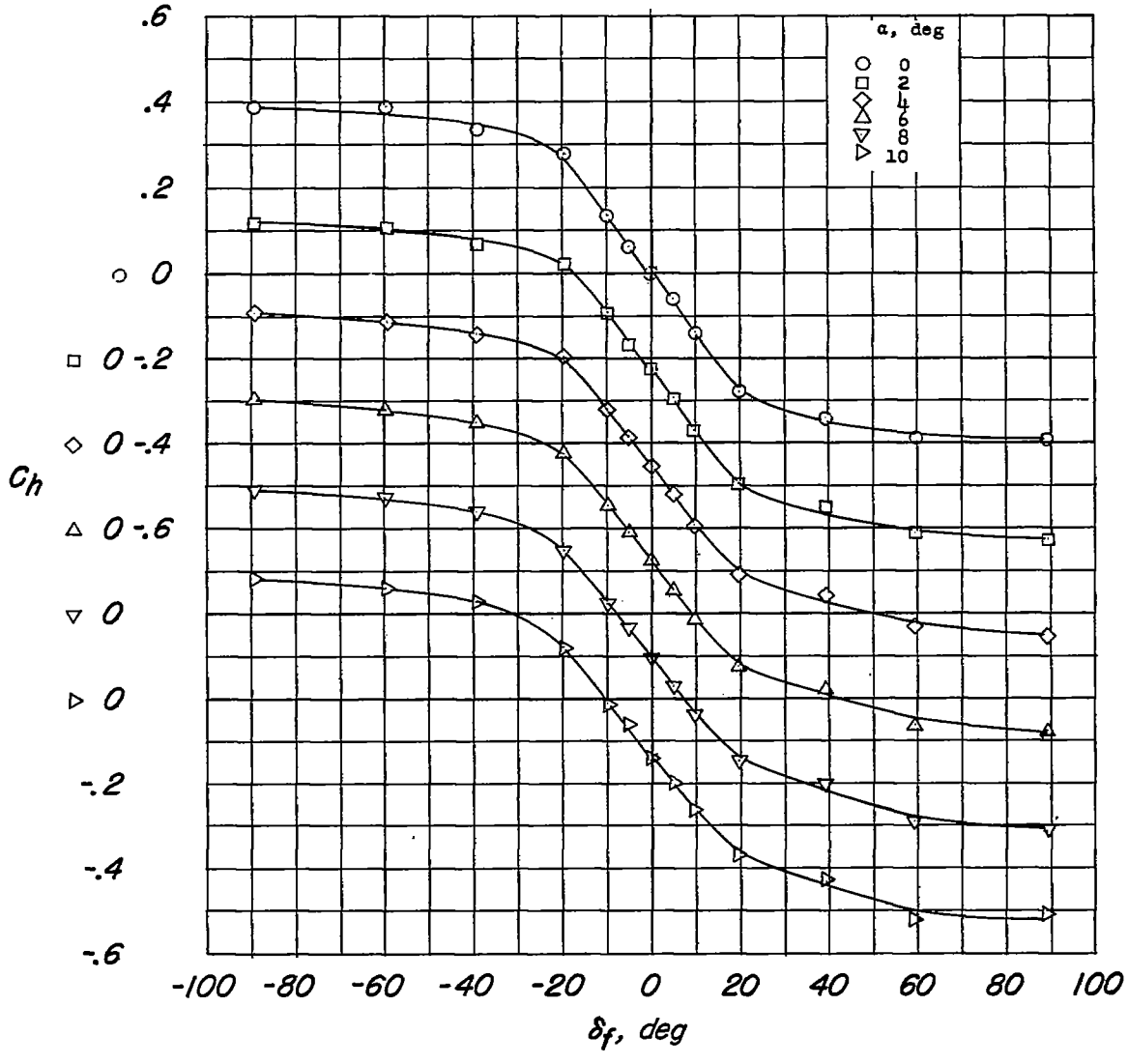

(i) M = 1.96.

Figure 6.- Concluded.

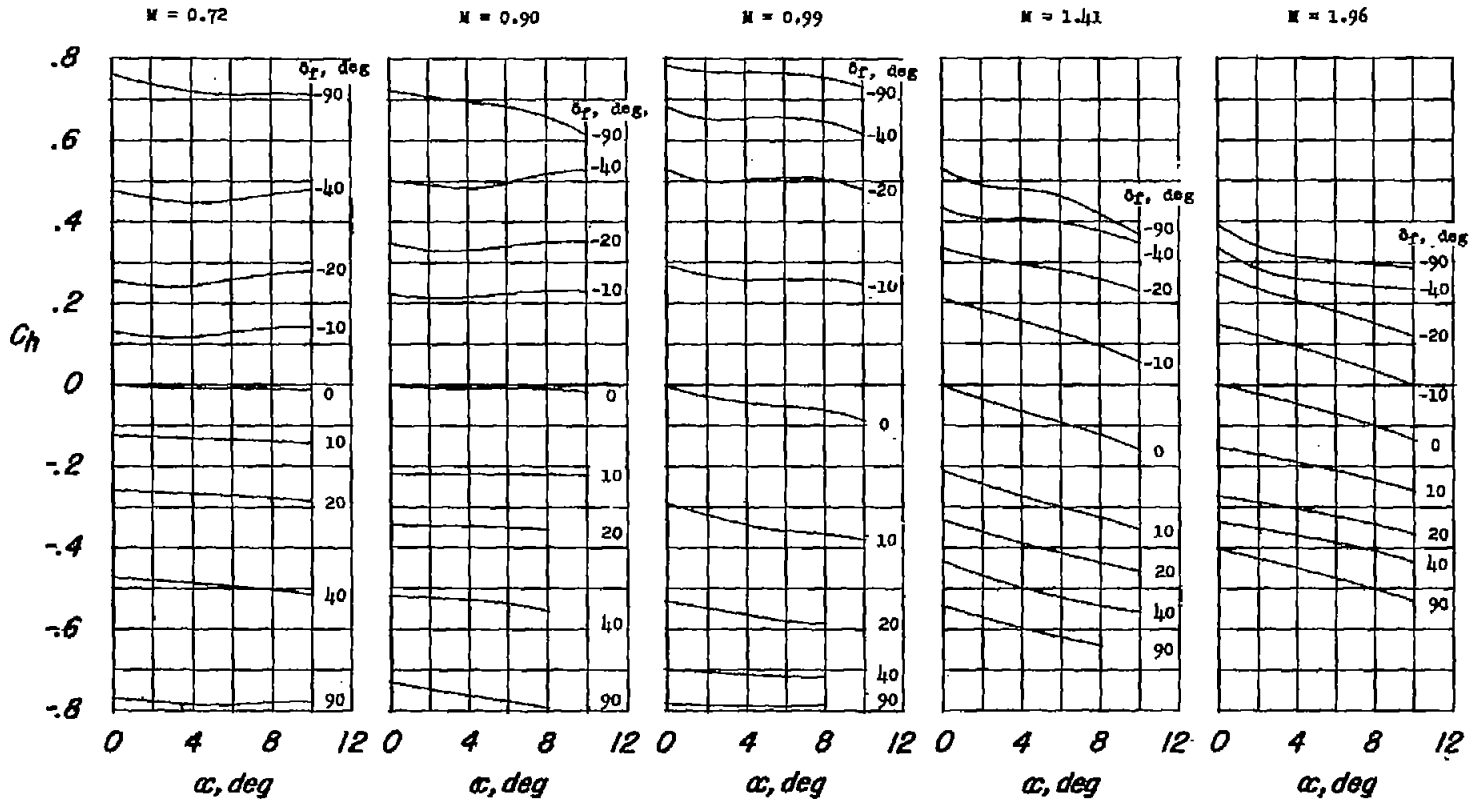

Figure 7.--Variation of hinge-moment coefficient with angle of attack at various control deflections.

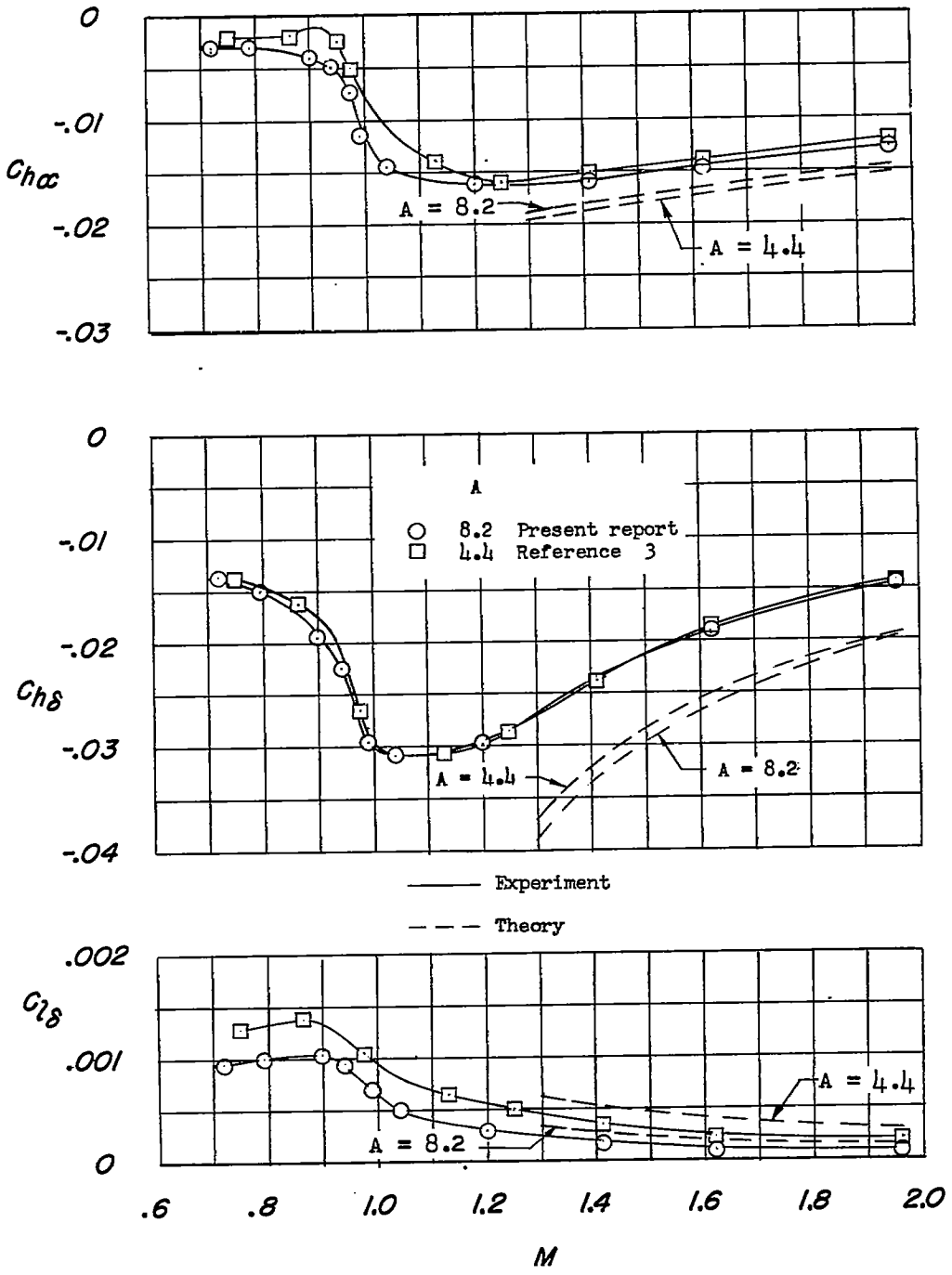

Figure 8.- Comparison of control parameters for two controls. $\delta_f = \alpha = 0^\circ$.

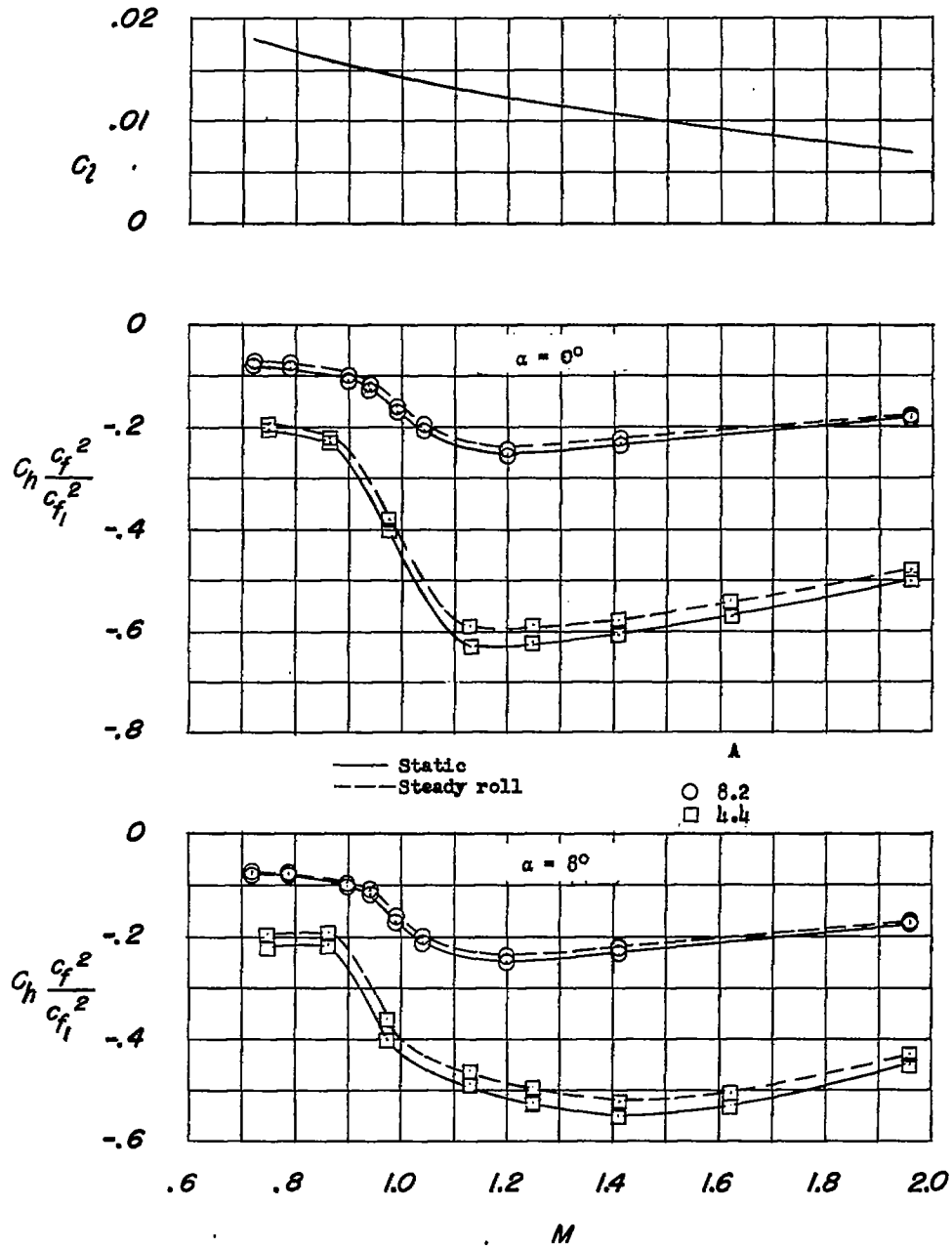

Figure 9.- Comparison of the variation with Mach number of the hinge-moment coefficient for two different aspect-ratio controls: Comparison is made at rolling moments required for roll rates of 3.5 radians per second for wings having 660 square feet of area and operating at 40,000 feet.

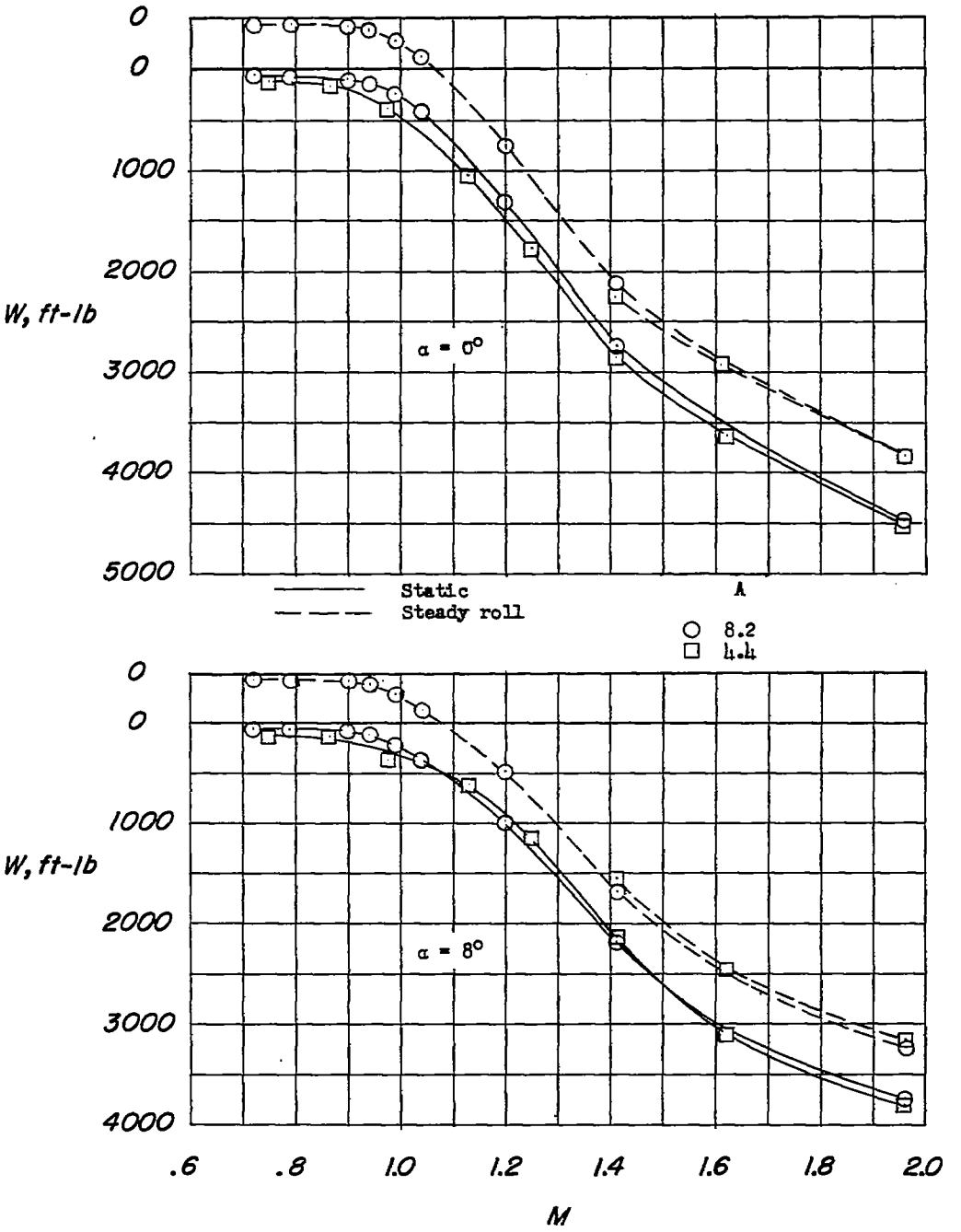

Figure 10.- Comparison of deflection work of two controls producing rolling moments required for roll rates of 3.5 radians per second for wings having 660 square feet of area and operating at 40,000 feet.

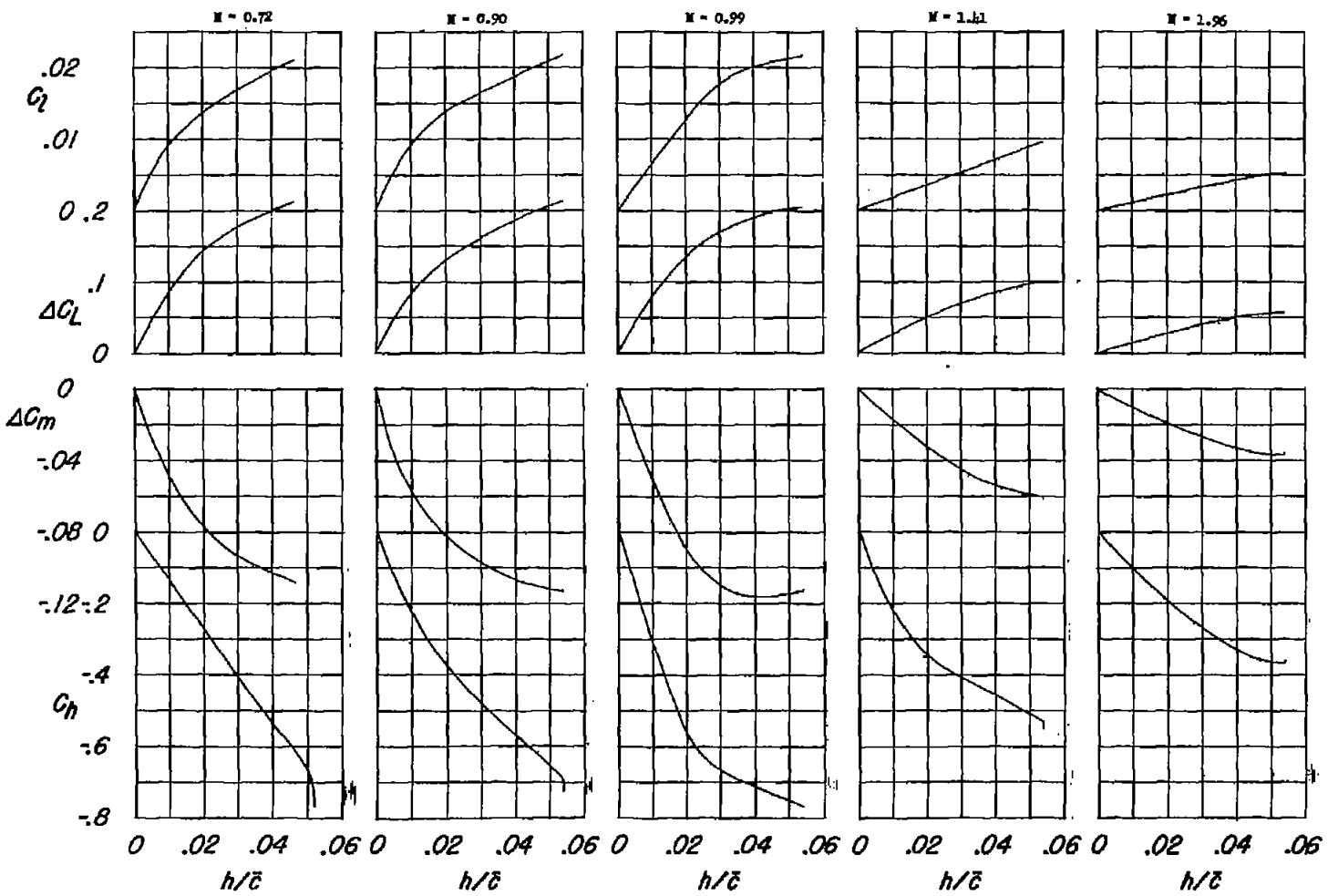

Figure 11.- Variation of C_l, ΔC_L, ΔC_m, and C_h with control deflection. $\alpha = 0^{\circ}$.

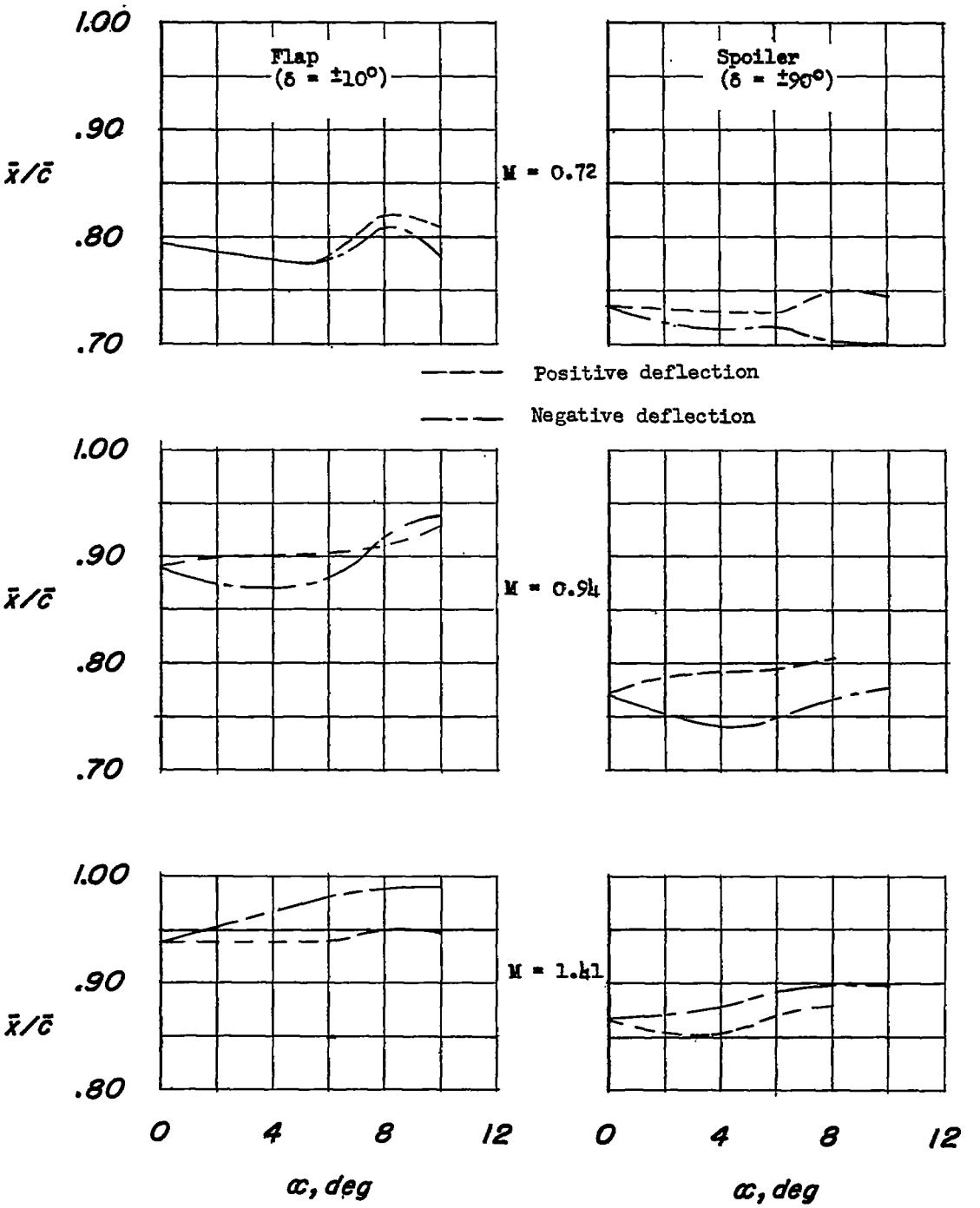

Figure 12.- Chordwise center-of-pressure location of incremental lift due to control deflected as a flap and as a spoiler.

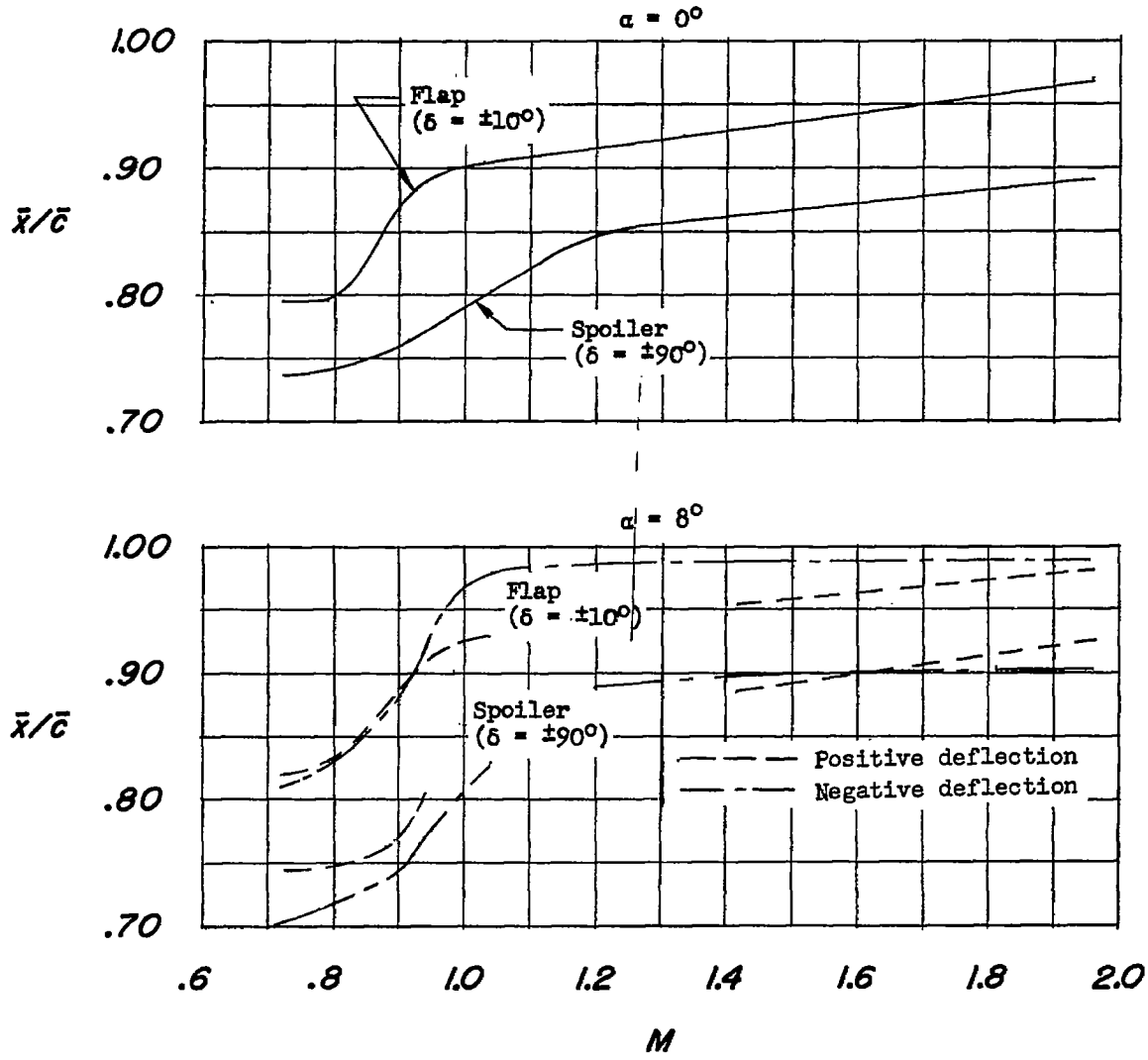

Figure 13.- Variation with Mach number of the chordwise location of the center of additional lift due to control deflected as a flap and as a spoiler.

NACA - Langley Field, Va.